AD NUMBER

ADB184823

NEW LIMITATION CHANGE

TO

Approved for public release, distribution unlimited

FROM

Distribution authorized to U.S. Gov't. agencies and their contractors; Administrative/Operational Use; AUG 1946. Other requests shall be referred to National Aeronautics and Space Administration, Washington, DC 20546.

AUTHORITY

NASA TR Server Website

NATIONAL ADVISORY COMMITTEE FOR AERONAUTICS

TECHNICAL NOTE

No. 1121

HIGH-SPEED INVESTIGATION OF SKIN

WRINKLES ON TWO NACA AIRFOILS

By Harold L. Robinson

Langley Memorial Aeronautical Laboratory
Langley Field, Va.

NACA

Washington
August 1946

DISCLAIMER NOTICE
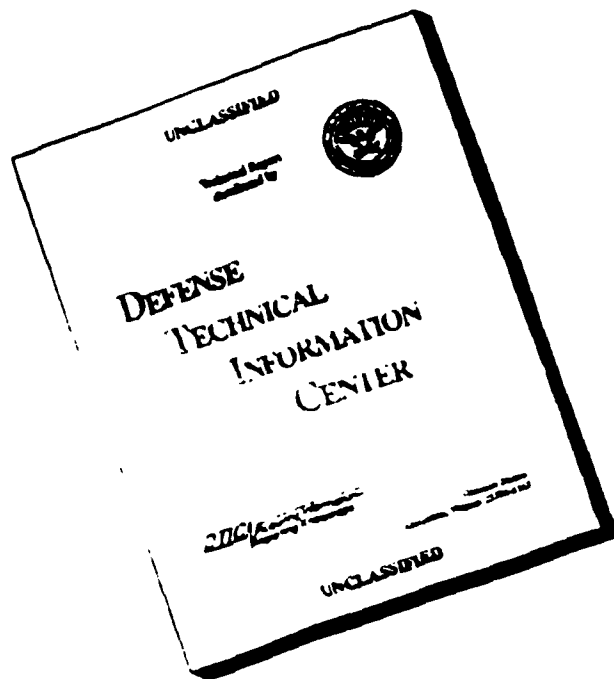
THIS DOCUMENT IS BEST QUALITY AVAILABLE. THE COPY FURNISHED TO DTIC CONTAINED A SIGNIFICANT NUMBER OF PAGES WHICH DO NOT REPRODUCE LEGIBLY.

NATIONAL ADVISORY COMMITTEE FOR AERONAUTICS

TECHNICAL NOTE NO. 1121

HIGH-SPEED INVESTIGATION OF SKIN

WRINKLES ON TWO NACA AIRFOILS

By Harold L. Robinson

SUMMARY

The effects on the aerodynamic characteristics of
skin wrinkles on the forward part of the upper surface
of two NACA airfoils have been investigated and the
results are compared with those obtained for the same
two airfoils in a smooth condition. The airfoils used
were the NACA 66,1-115 and 23015 sections. The wind-
tunnel investigation included speeds up to a Mach
number of 0.73.

The results showed that no appreciable change in
normal-force or pitching-moment characteristics over
the range of Mach number tested (0.25 to 0.73) was caused
by the wrinkle on an airfoil section. The drag for the
wrinkled configurations was greater than that for the
smooth configurations. The wrinkles caused a reduction
in the critical speed and a corresponding reduction in
the speed at which drag force breaks occur. The wake at
subcritical speeds spread an insignificant amount, and
the "shock spread" of the wake (the spread of the wake
due to shock on the airfoil) occurred at lower Mach
numbers for the wrinkled configurations than for the
smooth configurations. The results further indicated
that the span of the wrinkles tested had no effect on
the section aerodynamic characteristics.

A theoretical calculation of the pressure distri-
bution over the wrinkles was made and compared with a
low-speed pressure measurement.

INTRODUCTION

Airplane wings operating under high load conditions,
such as are encountered in gusts or pull-outs, may have

wrinkles developed on the skin. Although determining in
flight the profile of these wrinkles with a fair degree
of accuracy is impractical, determining in flight the
load condition under which these wrinkles occur is
relatively simple. Wrinkles similar to those observed
under flight conditions can thus be reproduced by
static-load tests. In order to determine the effects
of wrinkles of this type on the aerodynamic charac-
teristics of an airfoil, tests in the Langley 8-foot
high-speed tunnel were conducted with two representative
NACA airfoils having simulated typical wrinkles. The
wind-tunnel investigation included speeds up to a Mach
number of 0.73 and loads corresponding to conditions
simulating the lift coefficient required to produce
a 4g pull-out throughout the high-speed range for an
airplane having a wing loading of 40 pounds per square
foot and flying at an altitude of 20,000 feet.

The airfoils selected for the wind-tunnel investi-
gation were the NACA 66,1-115 and 23015 airfoils. The
NACA 66,1-115 airfoil is representative of airfoils
giving high critical speed, and the NACA 23015 airfoil
is representative of earlier conventional airfoils
having their peak negative pressure farther forward.

The profile of the wrinkles selected for the tests
were obtained from a full-scale static-load test specimen.
The wrinkles developed in the specimen consisted
principally of depressions relative to the original sur-
face so that the crests of the waves did not project
to any great extent above the original airfoil contour.
The chord of the specimen was 91 inches and the total
amplitude of the wrinkle was approximately 3/8 inch at
the section under the load at which the wrinkle profile
measurements were made. The wrinkles selected for the
present tests occurred in front of the forward spar of
the static-load test specimen; wrinkles developed behind
the forward spar were not included in the wind-tunnel
tests since it is believed that these wrinkles, because
of their large wave length, would not seriously show up
in flight.

Theoretical calculations of the pressure distri-
bution over the wrinkled NACA 66,1-115 airfoil were
made by a combination of the "slope method" of refer-
ence 1 and the Theodorsen-Garrick method of reference 2
for an angle of attack of 0°, and these theoretical

2

values are compared herein with the measured low-speed values.

SYMBOLS

P   pressure coefficient $\left(\dfrac{\text{Local pressure} - \text{Static pressure}}{\text{Dynamic pressure}}\right)$

c_l section lift coefficient

c_n section normal-force coefficient

$c_{m_{c/4}}$ section pitching-moment coefficient about quarter-chord point

c_{d_o} section profile-drag coefficient

α angle of attack

$\dfrac{\Delta V}{V}$ velocity-increment ratio

V   free-stream velocity

ΔV velocity increment above free-stream velocity

x   distance from airfoil nose parallel to chord, inches

y   distance from airfoil chord perpendicular to chord, inches; perpendicular to tunnel center line for wake-location data

Δy distance from smooth airfoil surface to wrinkled surface

X   coordinate of wrinkled surface on flat plate measured from airfoil nose, inches

Y   coordinate of wrinkled surface on flat plate measured from flat plate, inches $(Y = \Delta y)$

M   Mach number

c   airfoil chord, inches

3

Subscripts:

wp   wrinkle on flat plate

N   normal airfoil

T   wrinkle on airfoil surface

U   upper wake boundary

L   lower wake boundary

cr   critical, that is, value of variable when sonic
        velocity has just been attained in flow
        around airfoil

max   maximum

Other symbols used in appendix are defined as introduced.

APPARATUS AND PROCEDURE

The tests were conducted in the Langley 8-foot
high-speed tunnel, which has a single-return closed-
throat circular test section. The power available at
the time of the present tests limited speeds to $M = 0.73$.

The NACA 66,1-115 and 23015 airfoils, which had
24-inch chords, completely spanned the tunnel throat
as shown in figure 1. Two types of wrinkles having
different spans but the same chordwise shape were
investigated (figs. 2 to 4). These wrinkles were called
the long wrinkle and the short wrinkle and had spans
of 10 inches (0.417 chord) and 2 inches (0.0834 chord),
respectively. The wrinkled surface was simulated by
inserting blocks of the desired shape so that the leading
edge of the wrinkles was 0.5 inch (0.021 chord) behind
the airfoil leading edge, and the trailing edge of the
wrinkles was 5.5 inches (0.229 chord) behind the airfoil
leading edge. (See figs. 3 and 4.) The amplitudes of
the wrinkles were approximately 0.1 inch (0.00417 chord)
and the wave length was 2 inches (0.0834 chord). The
spanwise ends of the wrinkles were faired to the smooth
airfoil surface by fillets having a radius equal to the
departure of the wrinkled surface from the smooth surface.

The fillet at a valley was faired inward and the fillet at a peak was faired outward.

Carborundum dust that had a mean diameter of 0.005 inch was blown on a tacky shellac strip 3/32 inch (0.0039 chord) wide for the fixed-transition configuration. The leading edge of this transition strip was placed spanwise on the otherwise smooth model at the 0.021-chord station on the upper surface of the NACA 23015 airfoil. This location corresponds to the leading edge of the wrinkled surface. The NACA 66,1-115 airfoil was not tested in the fixed-transition configuration because drag and critical-speed data were available from unpublished tests previously conducted in the Langley 8-foot high-speed tunnel.

Profile drag was determined from measurements obtained by the wake-survey rake placed behind the airfoil (figs. 1 and 5) by the methods of reference 3. The wake-survey rake was supported on an auxiliary airfoil, or a horizontal strut, and could be moved from the tunnel vertical center plane to 24 inches on either side of this plane, as shown in figure 1. With the model set at $a = 0^\circ$, the total-pressure tubes of the rake were 37 inches (1.540 chords) behind the trailing edge of the NACA 66,1-115 airfoil and 19.81 inches (0.826 chord) behind the trailing edge of the NACA 23015 airfoil. In order to measure the profile drag of the wrinkled section, the rake was placed 15 inches spanwise from the center line of the model directly behind the midspan of the wrinkle; in order to measure the profile drag of the smooth-wing or fixed-transition configurations, the rake was placed symmetrically on the other side of the center line of the model. The total-pressure loss and the static pressures in the wake were measured on a multiple-tube integrating alcohol manometer. Great care was exercised to keep the model especially clean during the wake-survey tests.

Simultaneous pressure measurements were made at both spanwise stations for most of the runs. All the pressures were measured by photographing a multiple-tube tetrabromoethane manometer. Pressure data were obtained for the following configurations of the two NACA airfoils:

NACA 66,1-115 airfoil	NACA 23015 airfoil
Smooth wing	Smooth wing
Long wrinkle	Long wrinkle
Short wrinkle	Transition fixed at the 0.021-chord station on the upper surface

The wake-survey tests were not run simultaneously with the pressure measurements because the rake and strut absorb enough power to reduce appreciably the maximum tunnel speed. Drag data were obtained for the same configurations as were the pressure data except that drag was not measured for the short wrinkle of the NACA 66,1-115 airfoil.

RESULTS AND DISCUSSION

Pressure Distribution

Measured pressure distribution.- A representative group of the pressure distributions obtained are presented in figures 6 to 12 for the NACA 66,1-115 airfoil and in figures 13 to 18 for the NACA 23015 airfoil. The short-wrinkle pressure distributions and the long-wrinkle pressure distributions agreed quite closely; therefore only one group, for the long wrinkle, is presented in the present paper. A comparison of the two sets of data was expected to show the effects of spanwise flow that were believed to exist; the flow for both wrinkles was, however, apparently the same.

When comparisons were available, the pressure distributions for the fixed-transition and smooth-airfoil configurations are shown to agree quite closely (figs. 13 to 17); furthermore, for the range investigated the pressure recovery at the trailing edge behind the wrinkle is similar to that for the smooth airfoil, which indicates that any separation that does occur is not due to the wrinkle.

With increasing angle of attack the largest peak over the wrinkle on the NACA 66-series airfoil moves

to the more forward peaks (for example, figs. 7 and 11). This forward movement of the peak over the wrinkled airfoil is due to the forward movement of the peak over the normal airfoil. For the NACA 23015 airfoil (figs. 13 to 18), in which the pressure distribution of the normal airfoil does not have so sharp a peak at the nose at high angles of attack as that of the NACA 66,1-115 airfoil, the largest peak over the wrinkle remains at the same location regardless of the variation in angle of attack or speed.

Theoretical pressure distribution.- The pressures for the upper surface of the wrinkled NACA 66,1-115 airfoil were computed for an angle of attack of 0° by a combination of the slope method (reference 1) and the Theodorsen-Garrick method (reference 2). The slope method, which is given in the appendix, was used to compute the velocity-increment ratio over the wrinkle developed on a flat plate (fig. 4). This velocity-increment ratio was added to that obtained for the smooth airfoil (fig. 19) by the method of reference 2. The total velocity-increment ratio was then converted to pressure coefficient. In figure 20 the theoretical pressure coefficients are compared with the pressure coefficients measured at $a = 0^\circ$ and $M = 0.250$. Measuring the peak pressures when the gradients are sharp and steep is inherently difficult; also, local separation may occur. Both of these effects would cause the measured values to appear less severe than the calculated values at the peaks and valleys. The fairing for the measured pressure distribution is that customarily used but is, however, quite arbitrary. It is possible to fair through the measured pressure coefficients and obtain better agreement with the calculated curve than that shown in figure 20. The calculated values also are subject to small errors caused by fitting the equations of the wrinkled surface to the actual surface. Despite this difference in the fairing, the lift and the pitching-moment coefficients obtained from either the calculated or the measured pressure distributions agree quite closely because a peak difference is compensated by a valley difference.

Section Normal-Force Coefficient

The pressure distributions were integrated graphically to obtain the curves of section normal-force

coefficient that are presented in figures 21 and 22.
Some points for fairing these curves, where $M = 0.250$
and data were missing, were obtained by interpolation
from plots of c_n against α.

Figures 21 and 22 show that, for the range of
speed and angle of attack tested, the variation of c_n
with speed for the wrinkled, the fixed-transition, or
the smooth configurations remains the same. It may be
concluded, therefore, that no large detrimental effects
are caused by the wrinkle or the fixed-transition con-
figuration. In fact, at subcritical speeds a slight
increase in $c_{n_{max}}$ is possible for wrinkles of the size
investigated and in the location tested. This increase
probably results because transition is fixed at the
region of the wrinkle, and the turbulent boundary layer
that ensues may delay separation. Reference 4 shows
that, when small roughness was placed at several posi-
tions on the upper surface of the NACA 63(420)-422 air-
foil, an increase in $c_{l_{max}}$ $\left(\text{or } c_{n_{max}} \right)$ was obtained;
although, when roughness was placed on the nose of the
airfoil, a decrement to $c_{l_{max}}$ was experienced.

Section Pitching-Moment Coefficient

The section pitching-moment coefficients were
obtained by integrating the chordwise pressure distri-
bution to obtain the pitching moment about the quarter-
chord point; the small contribution of the chordwise
forces was neglected. The data for smooth and wrinkled
sections of the NACA 66,1-115 airfoil are presented in
figure 23. The section pitching-moment coefficients
for the smooth, the wrinkled, and the fixed-transition
configurations of the NACA 23015 airfoil are compared
in figure 24.

The effect of the wrinkle or of fixing transition
on the section pitching-moment coefficients is neither
consistent nor large. The wrinkle or fixing transition,
therefore, may be concluded to have no serious effect
on the pitching-moment characteristics of the airfoils
for the range investigated.

Section Profile-Drag Coefficient

The section profile-drag coefficients are presented for the NACA 66,1-115 airfoil in figure 25 and for the NACA 23015 airfoil in figure 26. The data for the fixed-transition configuration of the NACA 66,1-115 airfoil are from unpublished tests previously made in the Langley 8-foot high-speed tunnel.

Reference to figure 25 shows that the drag of the NACA 66,1-115 airfoil is increased for the wrinkled configuration. Through the subcritical speed range the drag increment due to the wrinkle is somewhat less than that caused by fixing transition on both surfaces. A perceptible drag rise (drag force break) is reached at lower speeds for the wrinkled configuration than for the smooth or the fixed-transition configuration.

Figure 26 shows that at subcritical speeds the drag increment due to the wrinkle on the NACA 23015 airfoil is equal to or slightly larger than the increment due to fixing transition on the upper surface only at the leading edge of the wrinkle. This equality indicated that the drag increment due to the wrinkle at subcritical speeds is mainly caused by moving the transition point to the region of the leading edge of the wrinkle. The drag rise for the wrinkled wing is seen to occur at a lower Mach number than the drag rise for the smooth wing or for the fixed-transition configuration.

Wake Location

Plots of point drag coefficient against vertical distance from the chord were used to obtain the wake boundary behind the airfoil. The position where the point-drag-coefficient gradient is first equal to zero is considered the boundary of the wake. This point is obtained from faired curves of point drag coefficient dc_{d_0}/dy against vertical distance y, typical curves of which are presented in figure 27.

The distance y, in inches, (fig. 5) was measured vertically from the airfoil chord extended to the wake-boundary measuring plane. The data were then reduced to nondimensional form by dividing y by the airfoil

chord c. This value y/c for the upper and the lower
limit of the wake is plotted against Mach number in
figure 28 for the NACA 66,1-115 airfoil. The wake
location for the NACA 23015 airfoil is presented in
figure 29.

In figures 28 and 29, the spread of the wake at
subcritical speeds is shown to be only slightly wider
for the wrinkled and the fixed-transition configurations
than for the smooth configuration. The "shock spread"
of the wake (the spread of the wake due to shock on
the airfoil), however, occurs at lower speeds for the
wrinkled configuration than for the smooth airfoil,
whereas it occurs at the same speed for the fixed-
transition airfoil as for the smooth airfoil.

Critical Speed

Critical speed is defined as the undisturbed air-
speed when sonic velocity is first attained in the flow
around an airfoil. The variation of critical Mach
number with section normal-force coefficient for the
NACA 66,1-115 airfoil is plotted in figure 30(a). The
single point for fixed transition was acquired from
unpublished data obtained in the Langley 6-foot high-
speed tunnel. The critical-speed data for the NACA 23015
airfoil are given in figure 30(b).

Figures 30(a) and 30(b) show that the critical
speeds for the fixed-transition and the smooth-wing
configurations are approximately equal to each other for
each of the airfoils tested. The critical speeds for
the wrinkled configuration are lower than those for the
smooth airfoil, the wrinkled NACA 23015 airfoil suffering
a more severe loss of critical speed than the wrinkled
NACA 66,1-115 airfoil.

In spite of the lower critical speed for the
wrinkled configurations, the normal force break appears
to occur at a speed at least as high for the wrinkled
configuration as for the smooth configuration. This
phenomenon indicates that localized compression shocks
will not necessarily cause normal force breaks to occur.
The rise in drag indicated by the curves of c_{d_0} against

M (figs. 25 and 26) for the wrinkled configurations,
however, does occur at the respective critical speeds.

10

Airplane Performance

Because no appreciable change in normal force or
pitching moment is caused by the wrinkle, there will be
no important changes in the stability of the airplane
at subcritical speeds. The speed of the airplane,
however, will be adversely affected by an increase in
drag when wrinkles occur on the airfoil surface. It
has previously been indicated that, at a given angle
of attack and Mach number, the wake of the wrinkled
section at supercritical speeds is wider than that of
the smooth section; therefore additional attention
should be given to the tail location when wing wrinkles
may occur in flight.

Wrinkles that would not cause the flow to separate,
formed farther back than the ones tested, will probably
have less effect on the airplane performance. An effect
of the wrinkle is to fix the transition point; hence
wrinkles farther back would not cause so much of the
airfoil to be subjected to the turbulent boundary-layer
flow, and the expected effect will necessarily be less
for the wrinkles that are farther back than the ones
tested.

CONCLUSIONS

The NACA 66,1-115 and 23015 airfoil sections in
smooth and wrinkled conditions have been investigated
in the Langley 8-foot high-speed tunnel. Effects of
skin wrinkles, which had spans of 10 inches and 2 inches,
on the forward part of the upper surface of the two air-
foils indicated the following conclusions:

1. The wrinkles did not appreciably change the
normal-force or the pitching-moment characteristics of
the airfoils.

2. The critical speed of the airfoil was lowered
by the wrinkle; however, the speed at which the section
pitching-moment and section normal-force curves break
remained unchanged for all practical purposes.

3. The drag increment due to the wrinkle at sub-
critical speeds was appreciable and the drag force

break for the wrinkled configurations occurred at lower Mach numbers than for the smooth configurations.

4. The wake at subcritical speed spread an insignificant amount due to the wrinkle, and the "shock spread" of the wake (the spread of the wake due to shock on the airfoil) occurred at lower Mach numbers for the wrinkled configurations than for the smooth configurations.

5. The wrinkles effectively fixed transition in the region of their leading edge.

6. The span of the wrinkles tested had no effect on section aerodynamic characteristics.

Langley Memorial Aeronautical Laboratory
        National Advisory Committee for Aeronautics
                Langley Field, Va., June 11, 1946

APPENDIX

EQUATIONS FOR COMPUTATION OF THE PRESSURE

DISTRIBUTION OVER A WRINKLED AIRFOIL

A particular application of the slope method (reference 1) is used to obtain equations for computation of the pressure distribution over a wrinkled airfoil. The equations apply for any surface that can be constructed by employing straight lines and circular arcs, provided the thickness ratio of the airfoils and of the wrinkles is not too large.

By use of reference 1 the velocity-increment ratio due to the wrinkles at $X = X_s$ is

$$\left(\frac{\Delta V_{wp}}{V}\right)_{X_s} = \frac{1}{\pi} \int_0^c \frac{\frac{dY}{dX}\, dX}{X_s - X} \tag{1}$$

The wrinkle may be expressed, in regions, as straight-line and circular-arc functions of X. (See fig. 4.) It is convenient therefore to express equation (1) as follows:

$$\left(\frac{\Delta V_{wp}}{V}\right)_{X_s} = \sum_{i=1}^{g} \frac{1}{\pi} \int_{X_{i-1}}^{X_i} \frac{\frac{dY}{dX}\, dX}{X_s - X} \tag{2}$$

where $X_0 = 0$ inch and $X_g = 24$ inches. For a straight-line part of the wrinkle between $i - 1$ and i

$$\frac{1}{\pi} \int_{X_{i-1}}^{X_i} \frac{\frac{dY}{dX}\, dX}{X_s - X} = -\frac{1}{\pi} \frac{Y_i - Y_{i-1}}{X_i - X_{i-1}} \Big[\log_e (X_s - X)\Big]_{X_{i-1}}^{X_i} \tag{3}$$

13

For a circular-arc part of the wrinkle between 1 - 1
and 1

$$\frac{1}{\pi}\int_{X_{i-1}}^{X_1} \frac{\frac{dY}{dX}\,dX}{X_s - X} = \pm\left(\frac{1}{\pi}\beta + A\right) \qquad \text{if } \lambda < 0 \qquad (4a)$$

$$= \pm\left(\frac{1}{\pi}\beta + B\right) \qquad \text{if } \lambda > 0 \qquad (4b)$$

$$= \pm\left(\frac{1}{\pi}\beta + G\right) \qquad \text{if } \lambda = 0 \qquad (4c)$$

where

$$\beta = \left[\sin^{-1}\frac{X - c_X}{r}\right]_{X_{i-1}}^{X_1}$$

$$A = -\frac{k}{\pi}\frac{1}{\sqrt{-\lambda}}\left[\theta\right]_{X_{i-1}}^{X_1}$$

$$B = \frac{k}{\pi\sqrt{\lambda}}\left[\log_e\left(\frac{w + \sqrt{\lambda}}{X - X_s} + \frac{k}{\sqrt{\lambda}}\right)\right]_{X_{i-1}}^{X_1}$$

$$G = \frac{1}{\pi}\left[\frac{w}{X - X_s}\right]_{X_{i-1}}^{X_1}$$

and

$$\left[\theta\right]_{X_{i-1}}^{X_1} = \left[\sin^{-1}\left(\frac{k(X - X_s) + \lambda}{r(X - X_s)}\right)\right]_{X_{i-1}}^{X_1}$$

$$w = \sqrt{\lambda + 2k(X - X_s) - (X - X_s)^2}$$

$$\lambda = r^2 - k^2$$

$$k = c_X - X_s$$

c_X abscissa of arc center

r radius of arc

i number assigned to tangent points

g number of tangent points (16 for this application)

X_s point for which $\dfrac{\Delta V}{V}$ is being computed

If the circular arc is concave upward the negative sign is used in equation (4).

When equations (3) and (4) are integrated and added as indicated in equation (2), the velocity-increment ratio due to the wrinkle is obtained for any desired point $X = X_s$. This velocity-increment ratio is then added to the velocity-increment ratio for the smooth wing $\dfrac{\Delta V_N}{V}$ at $X = X_s$, which was obtained from figure 19 by the method of reference 2. The total velocity-increment ratio $\dfrac{\Delta V_T}{V}$ for the wrinkle and smooth section was then converted to pressure coefficient by the incompressible-flow relation

$$P = -\frac{\Delta V_T}{V}\left(\frac{\Delta V_T}{V} + 2\right) \tag{5}$$

A sample computation of P for $X_s = 1.274$ is given in table I.

REFERENCES

1. Wright, Ray H.: Estimation of Pressures on Cockpit
   Canopies, Gun Turrets, Blisters, and Similar
   Protuberances. NACA ACR No. L4E10, 1944.

2. Theodorsen, T., and Garrick, I. E.: General Potential
   Theory of Arbitrary Wing Sections. NACA Rep.
   No. 452, 1933.

3. Baals, Donald D., and Mourhess, Mary J.: Numerical
   Evaluation of the Wake-Survey Equations for
   Subsonic Flow Including the Effect of Energy
   Addition. NACA ARR No. L5H27, 1945.

4. Abbott, Frank T., Jr., and Turner, Harold R., Jr.:
   The Effects of Roughness at High Reynolds Numbers
   on the Lift and Drag Characteristics of Three
   Thick Airfoils. NACA ACR No. L4H21, 1944.

TABLE I

SAMPLE COMPUTATION OF P FOR $X_s = 1.274$ INCHES

(5.31 PERCENT CHORD)

Region	$\dfrac{1}{\pi}\displaystyle\int_{X_{i-1}}^{X_i} \dfrac{\frac{dY}{dX}\,dX}{X_s - X}$
0 - 1	0
1 - 2	-.00332
2 - 3	-.00628
3 - 4	-.10348
4 - 5	-.06570
5 - 6	-.00717
6 - 7	.01070
7 - 8	.01158
8 - 9	0
9 - 10	.00099
10 - 11	.00817
11 - 12	-.00151
12 - 13	-.00499
13 - 14	-.00183
14 - 15	.00114
15 - 16	0
$\displaystyle\sum_{i=1}^{16}$	-0.2282

$$\frac{\Delta V_{wp}}{V} = -0.2282$$

$$\frac{\Delta V_N}{V} = 0.1270 \text{ (from fig. 19)}$$

$$\frac{\Delta V_T}{V} = \frac{\Delta V_{wp}}{V} + \frac{\Delta V_N}{V} = -0.1012$$

$$P = -\frac{\Delta V_T}{V}\left(\frac{\Delta V_T}{V} + 2\right) = 0.192$$

NATIONAL ADVISORY
COMMITTEE FOR AERONAUTICS

17

Fig. 1
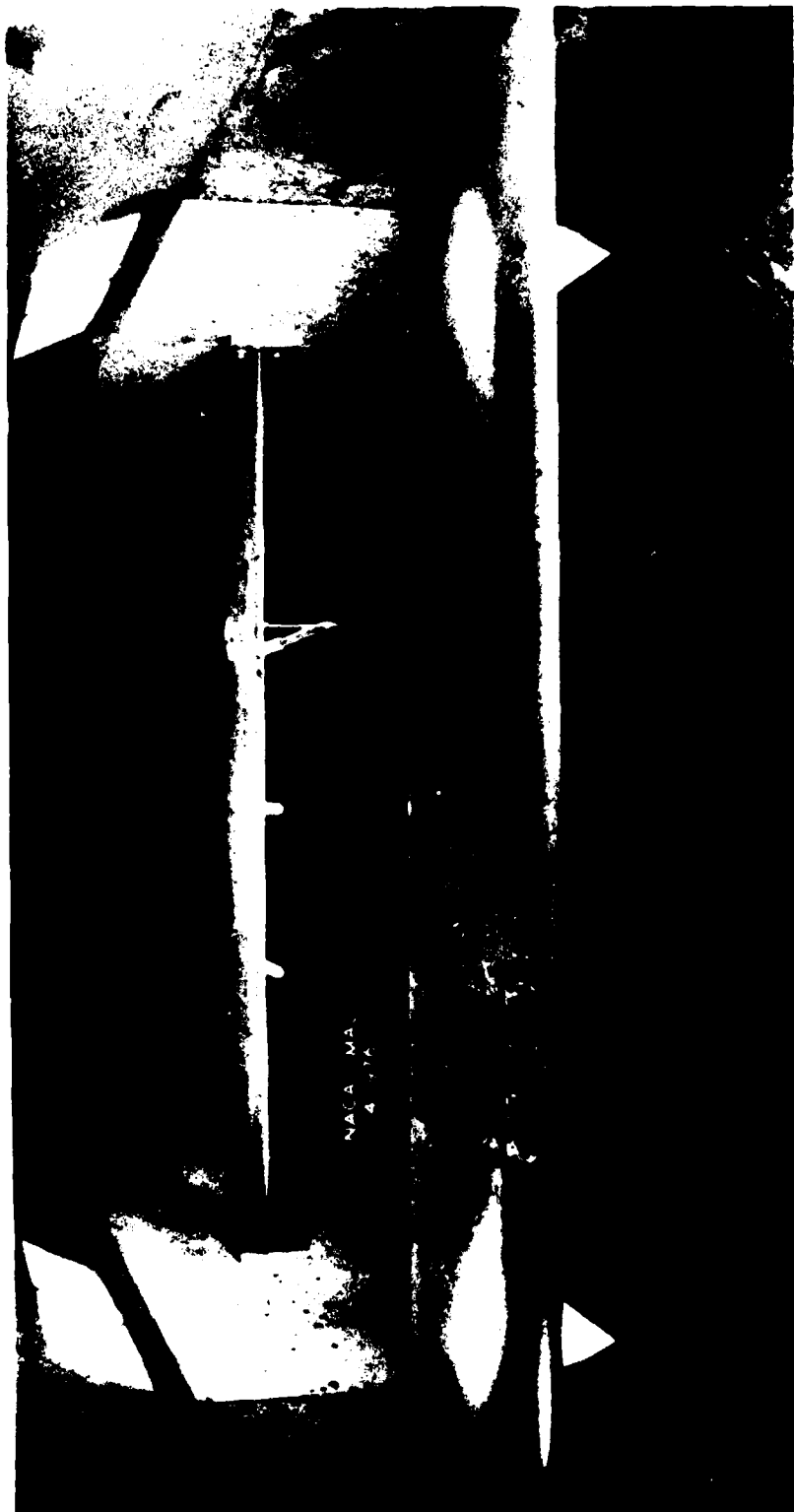
Figure 1.- Wing and rake in the Langley 8-foot high-speed tunnel.

NACA 23015 section

NACA 66,1-115 section

NATIONAL ADVISORY
COMMITTEE FOR AERONAUTICS

Scale, in.
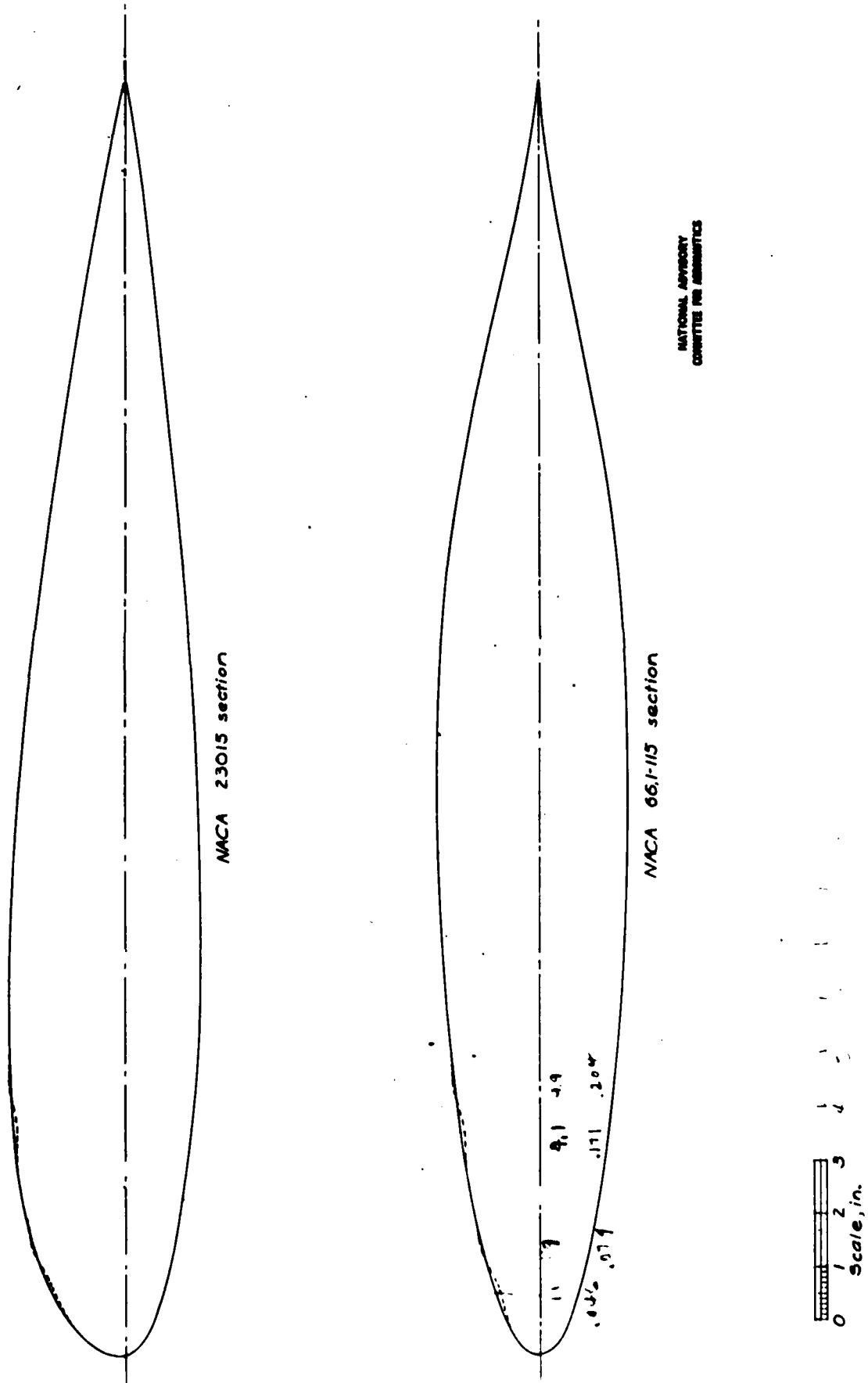
Figure 2.— Comparison of the NACA 23015 and the NACA 66,1-115 sections.

POSITION OF ORIFICES IN AIRFOIL

TUNNEL WALL

AIRFOIL-WRINKLE INSERTS

SECTION BB-WRINKLED WING

CROSS SECTION OF SHORT WRINKLE IS THE SAME
AS CROSS SECTION OF LONG WRINKLE

LONG
WRINKLE

SHORT WRINKLE

SECTION THRU PEAK
SECTION C-C

SECTION THRU VALLEY
SECTION A-A
SPANWISE FAIRING AT BLOCK
AND WING INTERSECTION

SHORT-WRINKLE BLOCKS INSERTED IN
SAME LOCATION AS LONG-WRINKLE BLOCKS
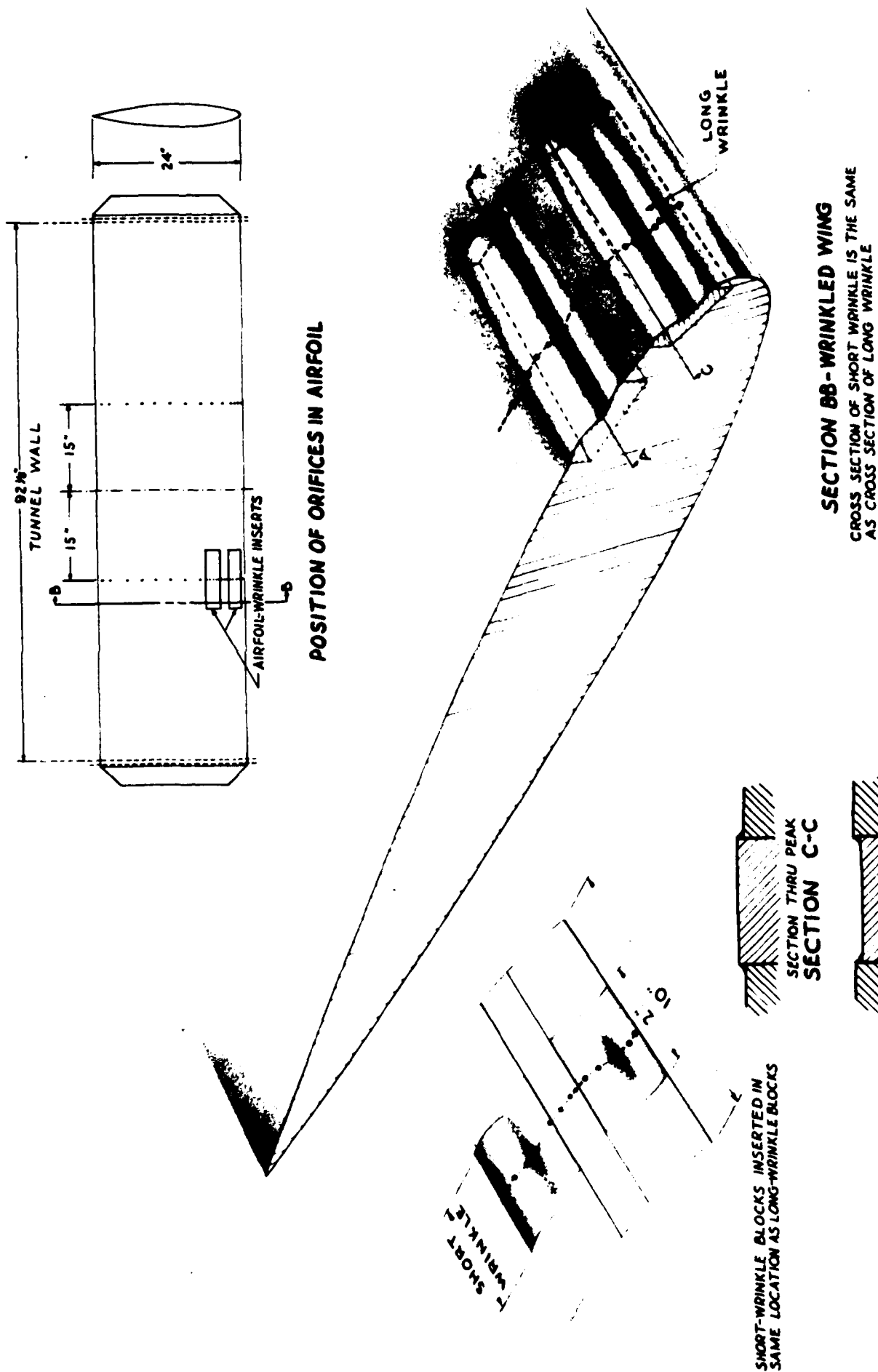
NATIONAL ADVISORY
COMMITTEE FOR AERONAUTICS.

FIGURE 3.— WRINKLE LOCATION AND DETAILS.
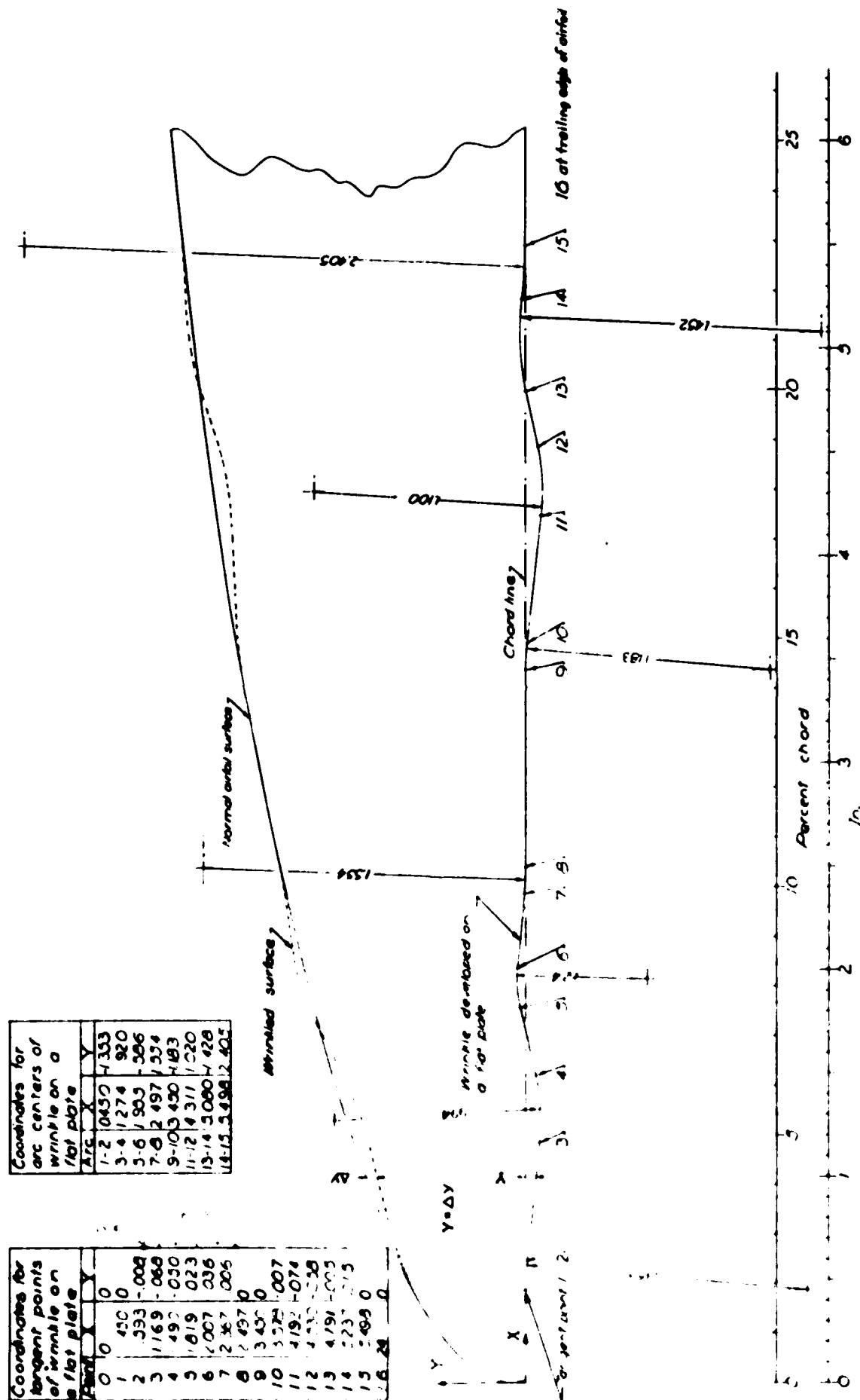
Figure 4 - Upper leading edge of the NACA 66,1-115 airfoil and dimensions of the wrinkle used for the theoretical pressure distribution. All dimensions are in inches unless otherwise noted.
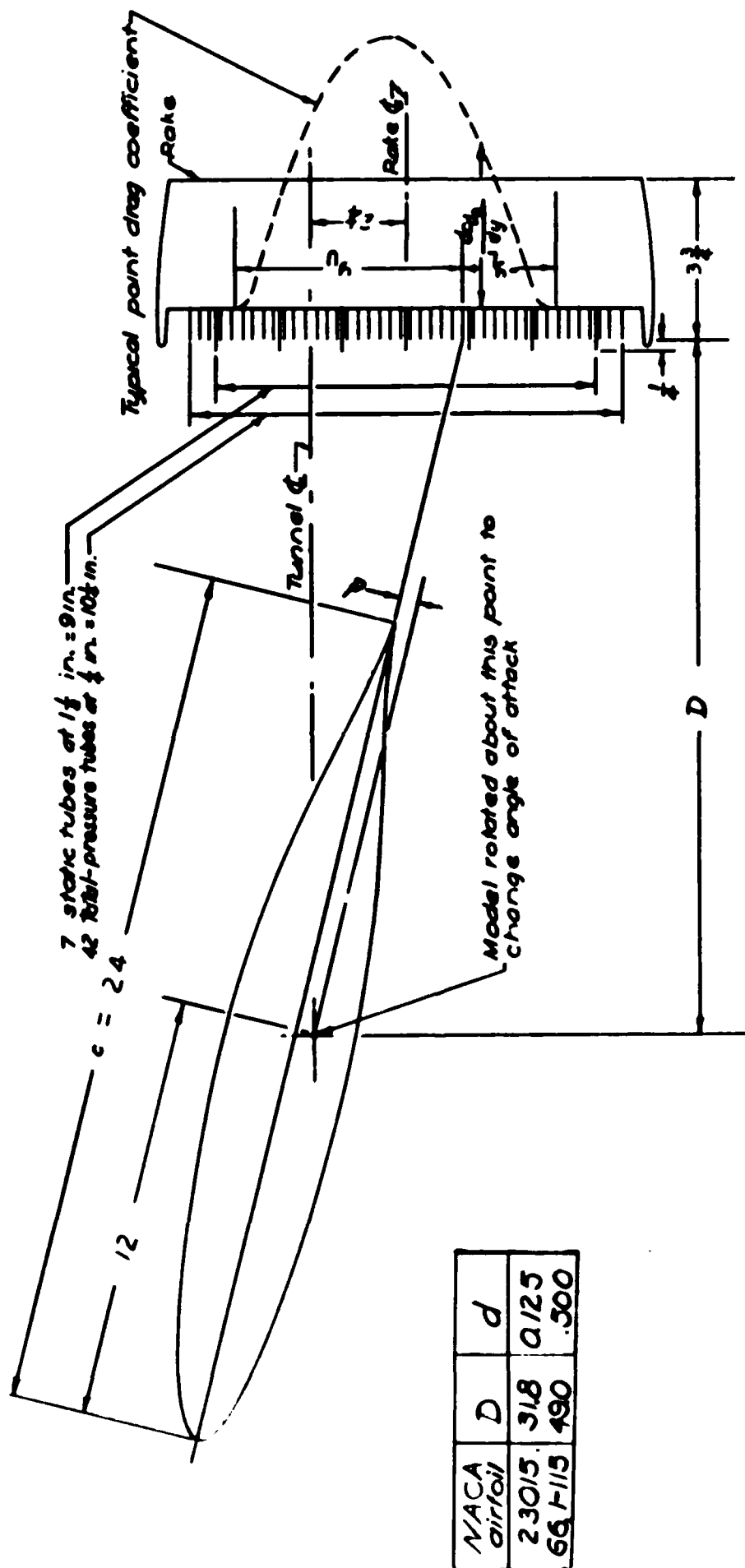
Fig. 5   NACA TN No. 1121

Figure 5.- Schematic diagram of wake-survey apparatus.
All dimensions are in inches.
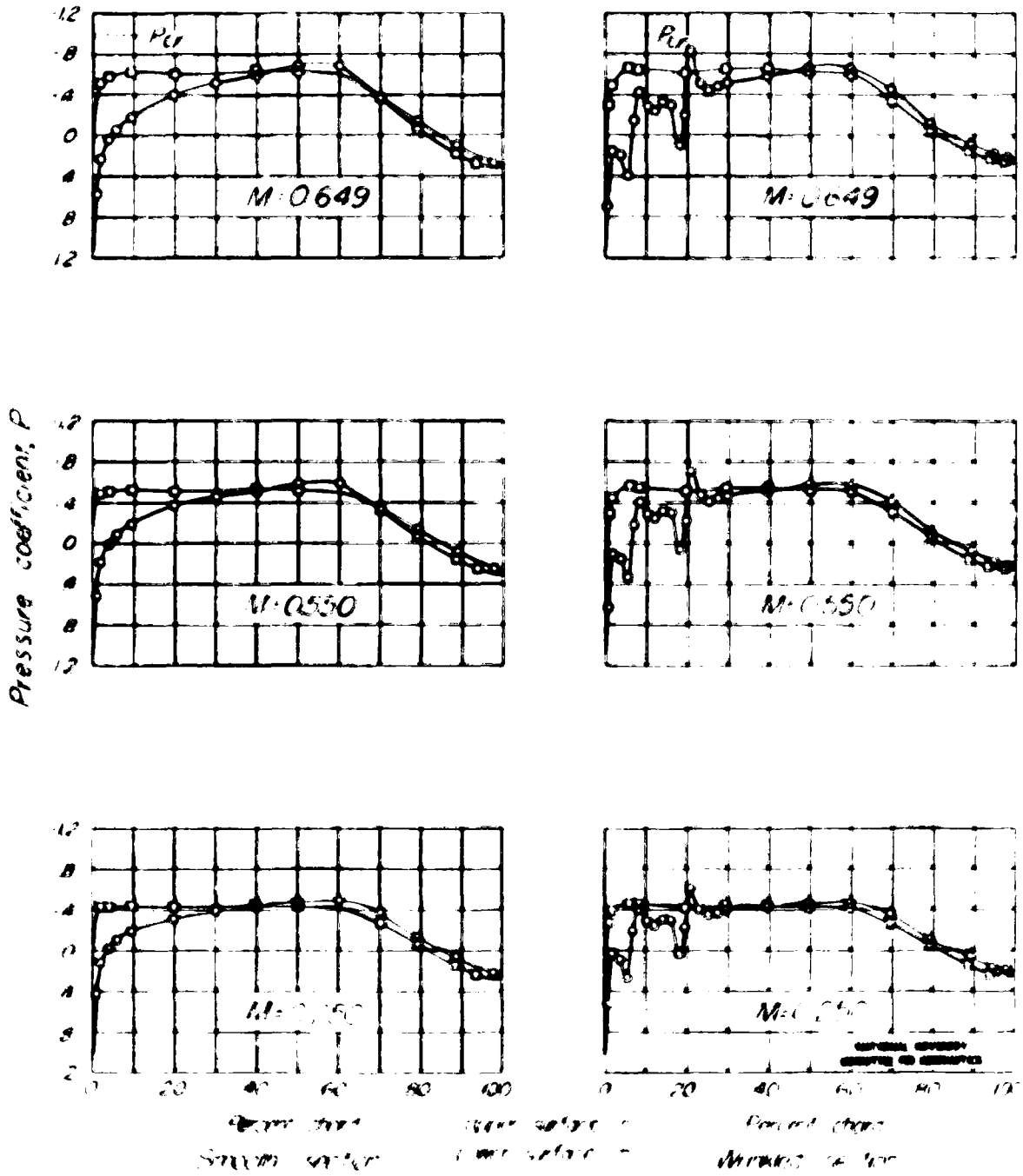
Figure 6 - Pressure distribution over NACA 65,1-115 airfoil.

Fig. 6 conc.

NACA TN No. 1121
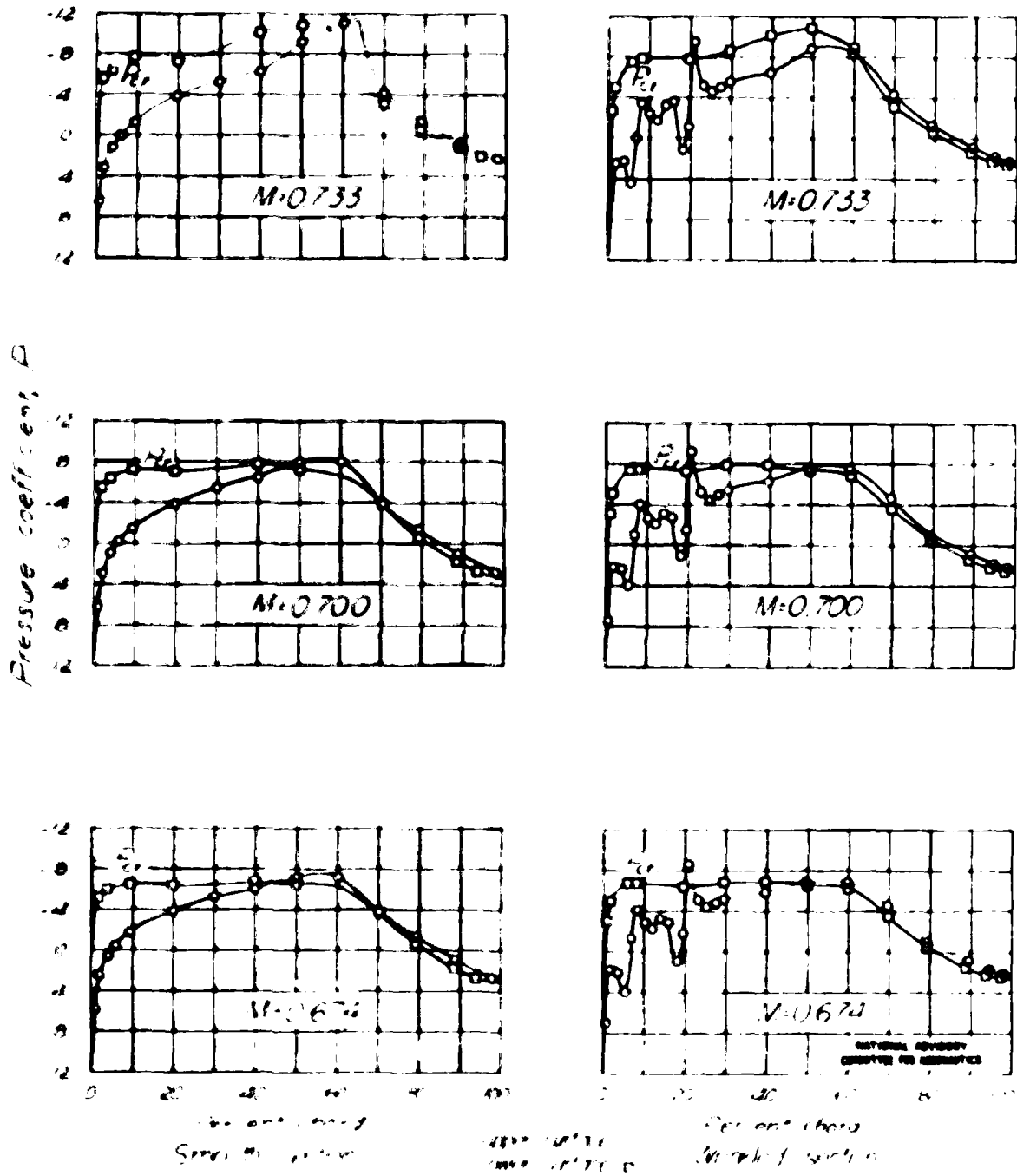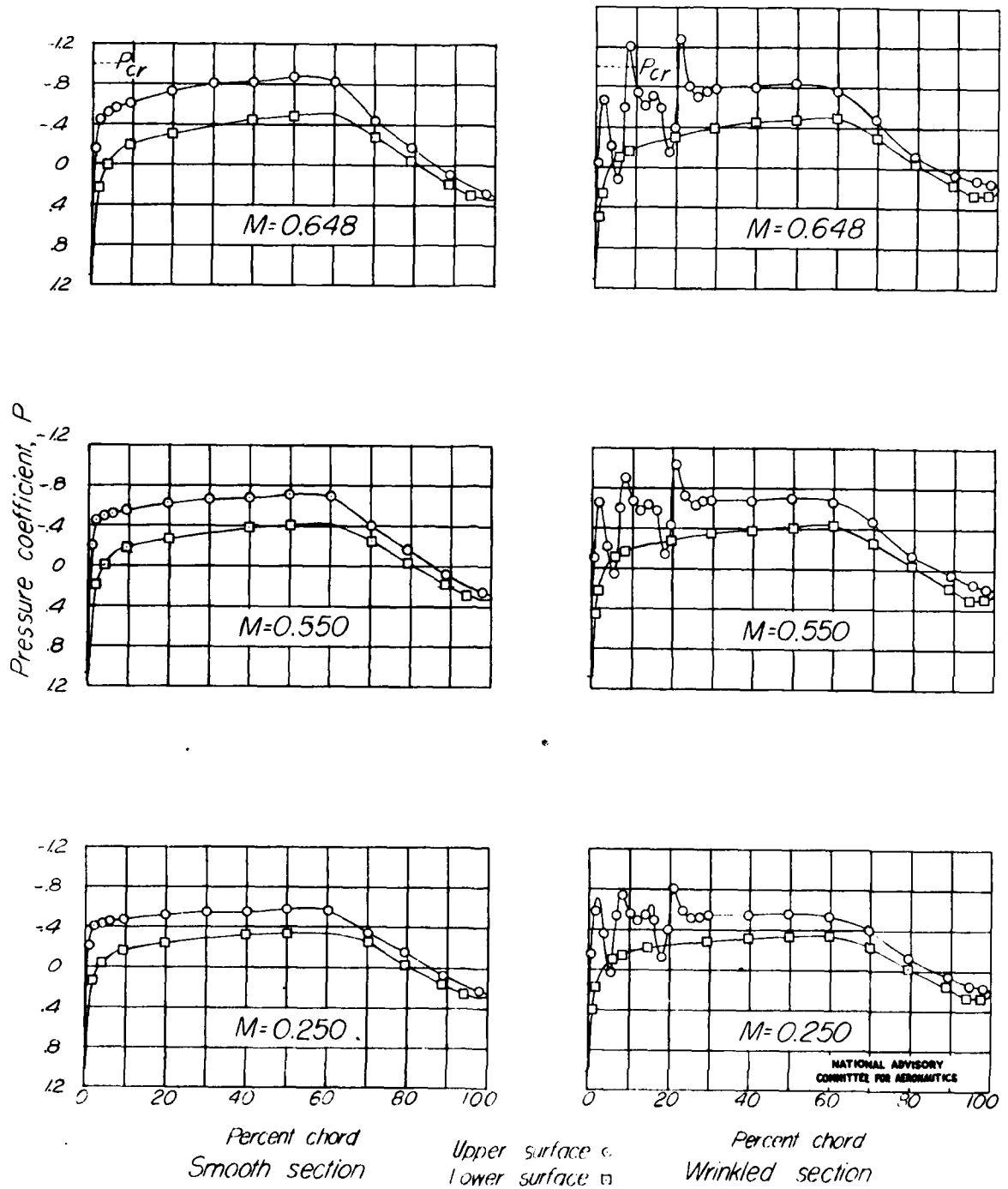
Figure 6.- Concluded.

Figure 7.-Pressure distribution over NACA 66,1-115 airfoil. α = 1°.

Fig. 7 conc.   NACA TN No. 1121
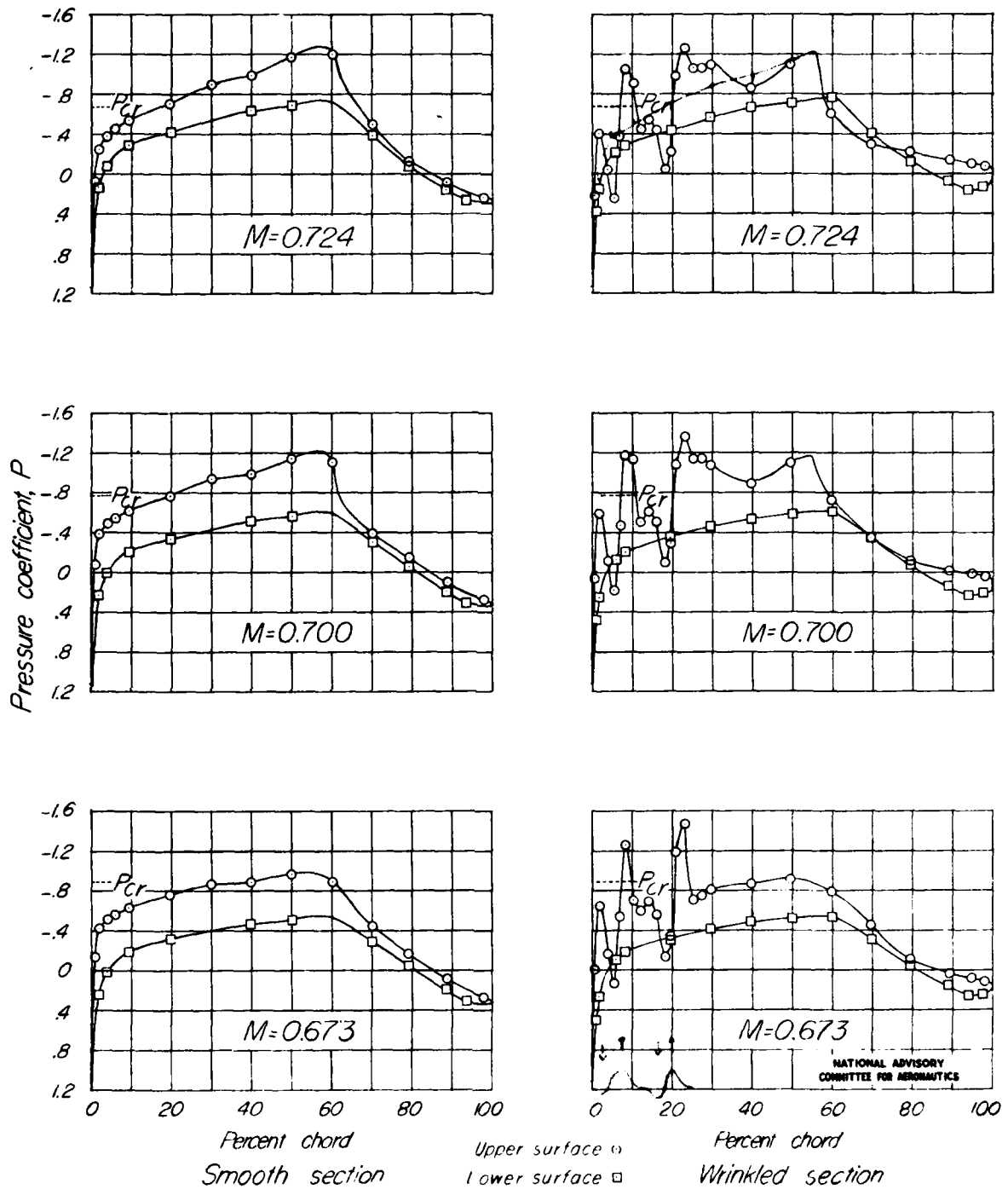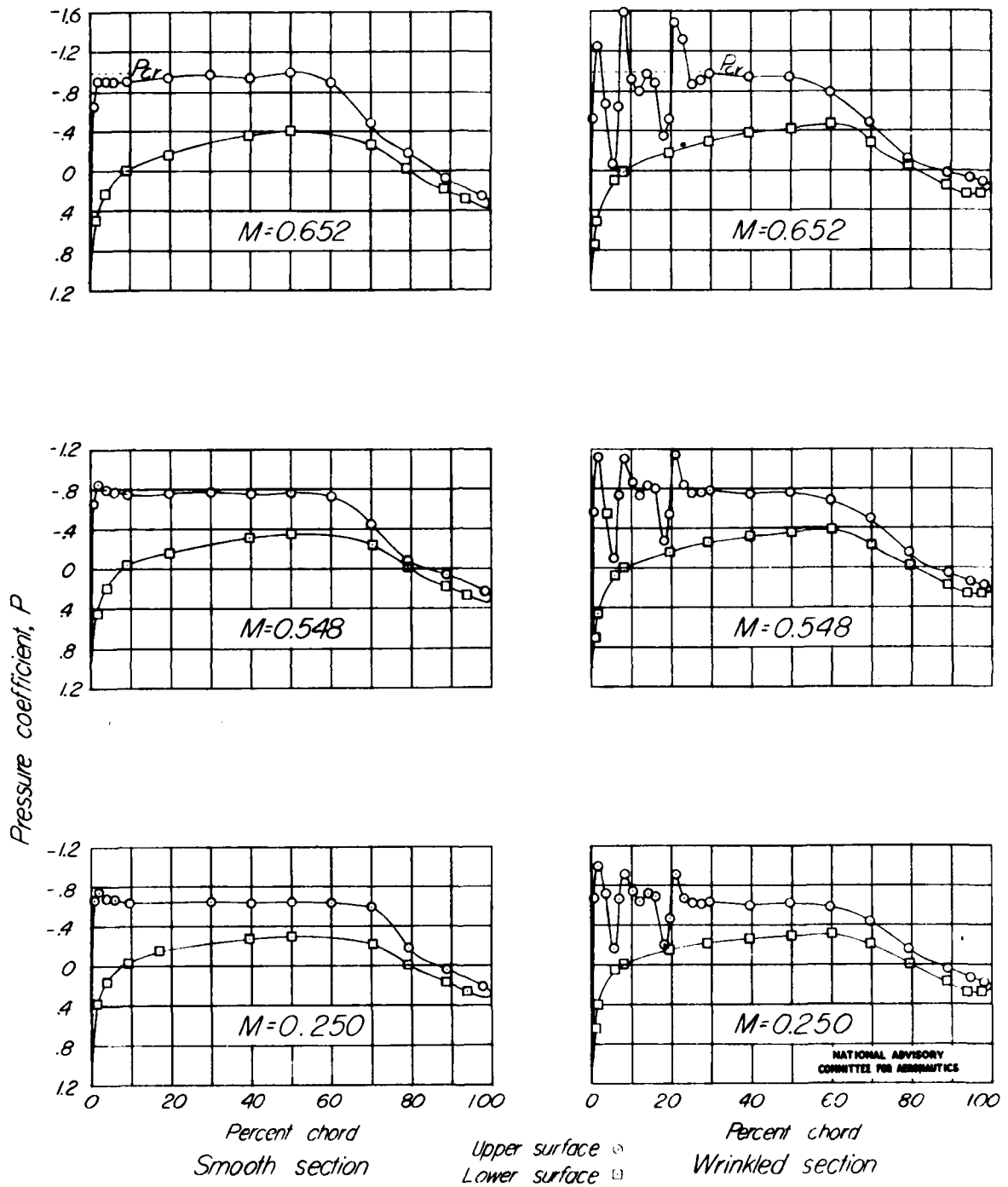
Figure 7.-Concluded.

Figure 8.- Pressure distribution over NACA 66,1-115 airfoil. $\alpha = 2°$

Fig. 8 conc.   NACA TN No. 1121
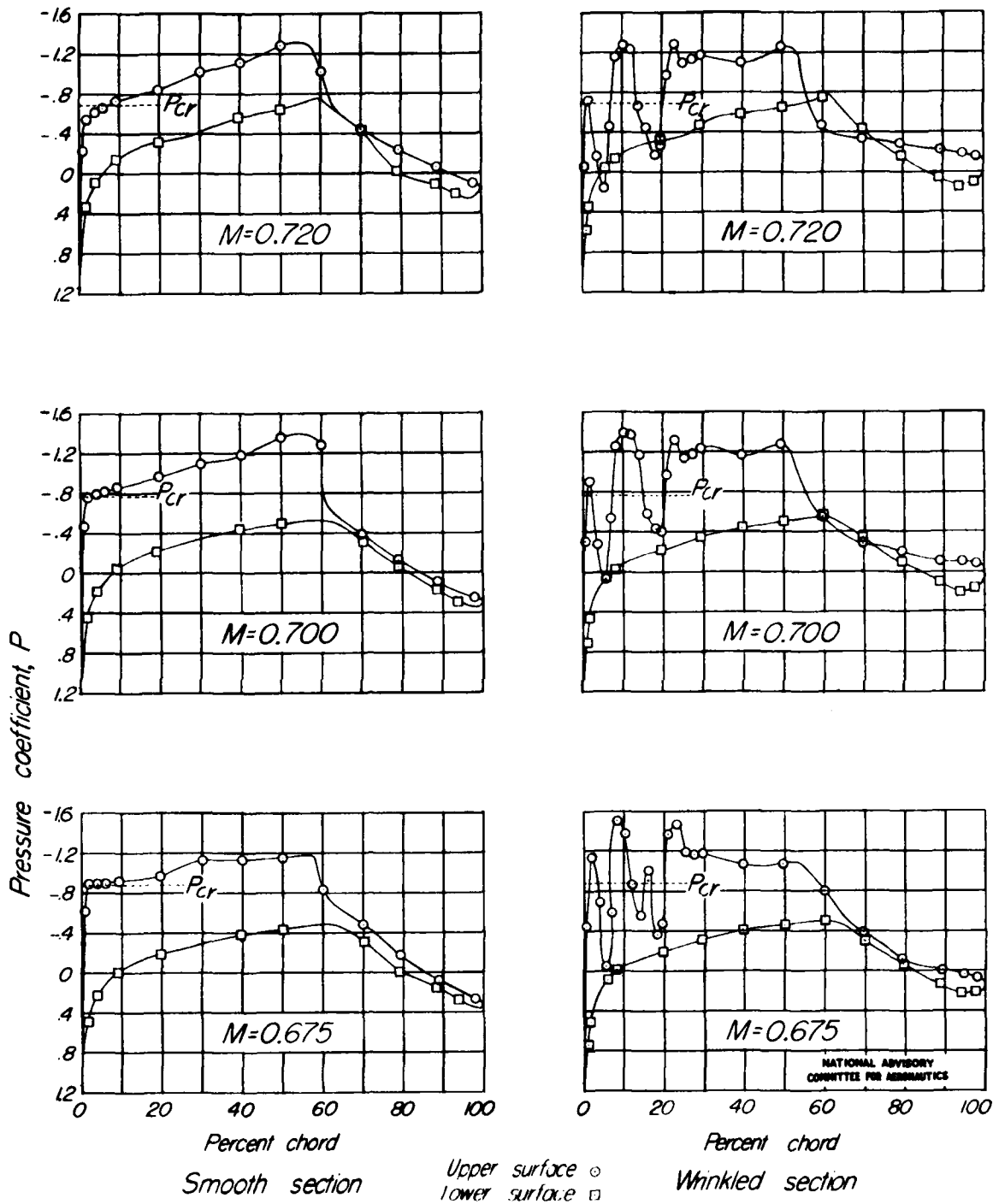
Figure 8. - Concluded.
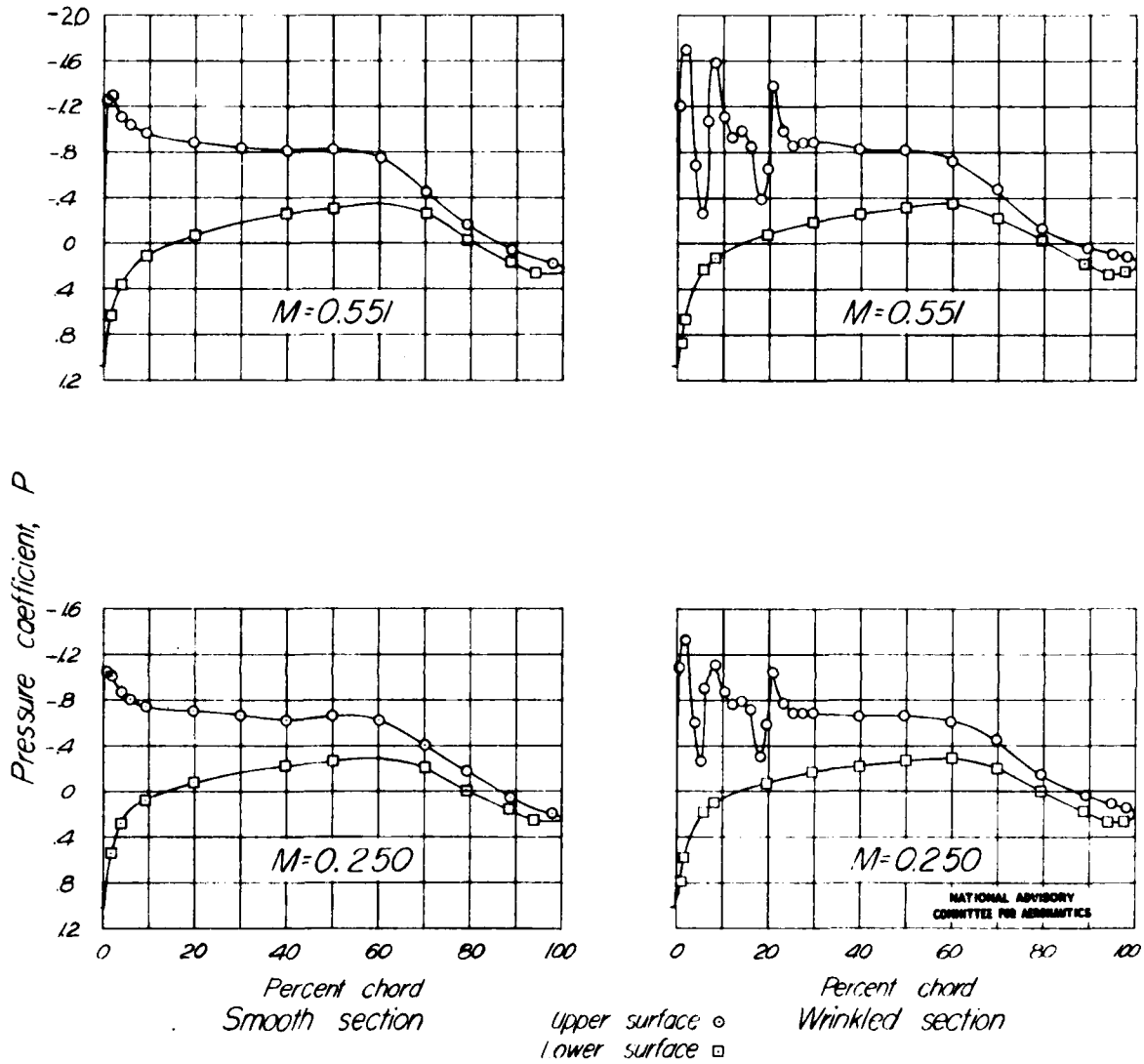
Figure 9.-Pressure distribution over NACA 66,1-115 airfoil. α=3°

Fig. 10   NACA TN No. 1121
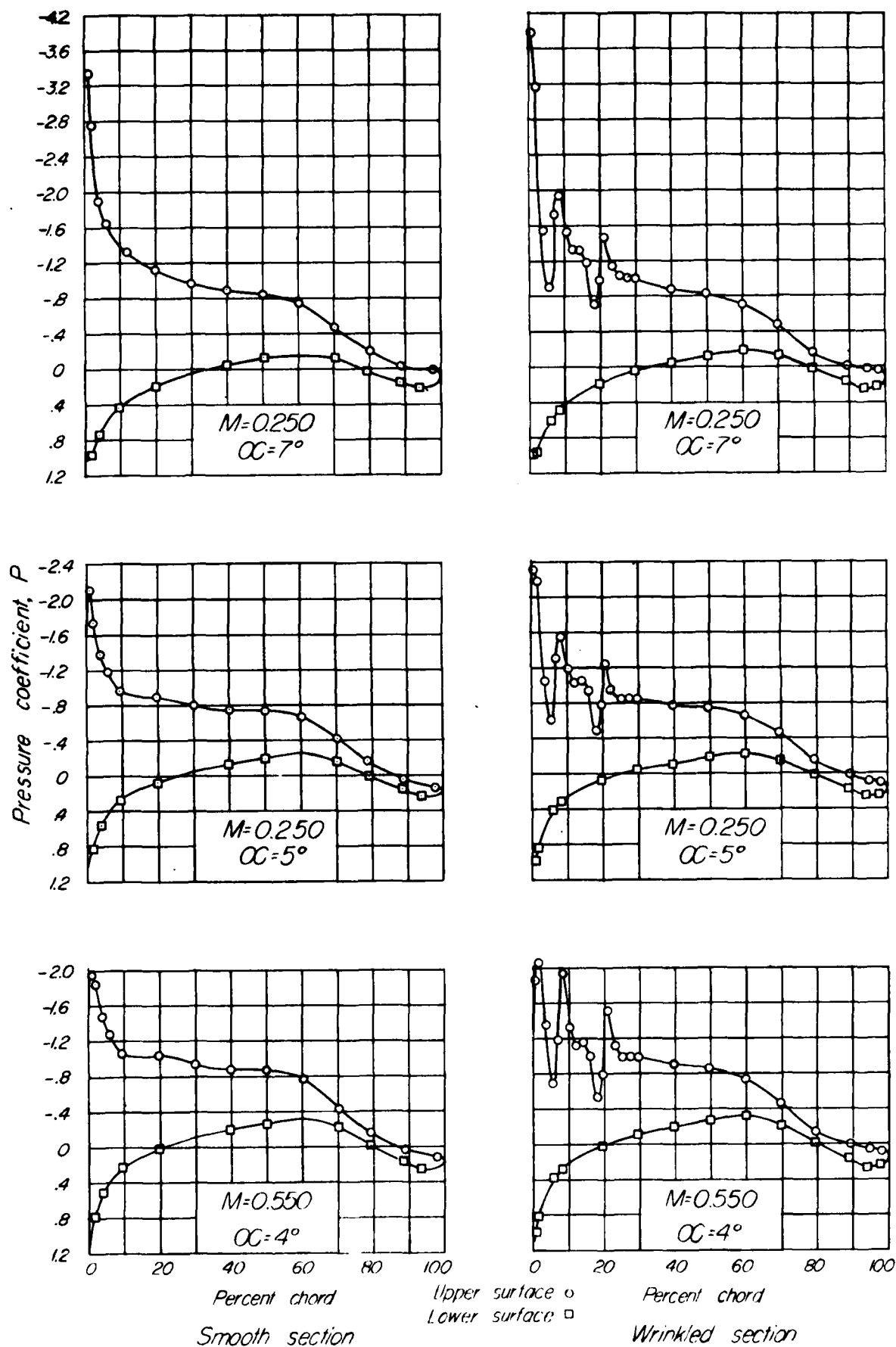
Figure 10.-Pressure distribution over NACA 66,1-115 airfoil.
$\alpha = 4°, 5°,$ and $7°$
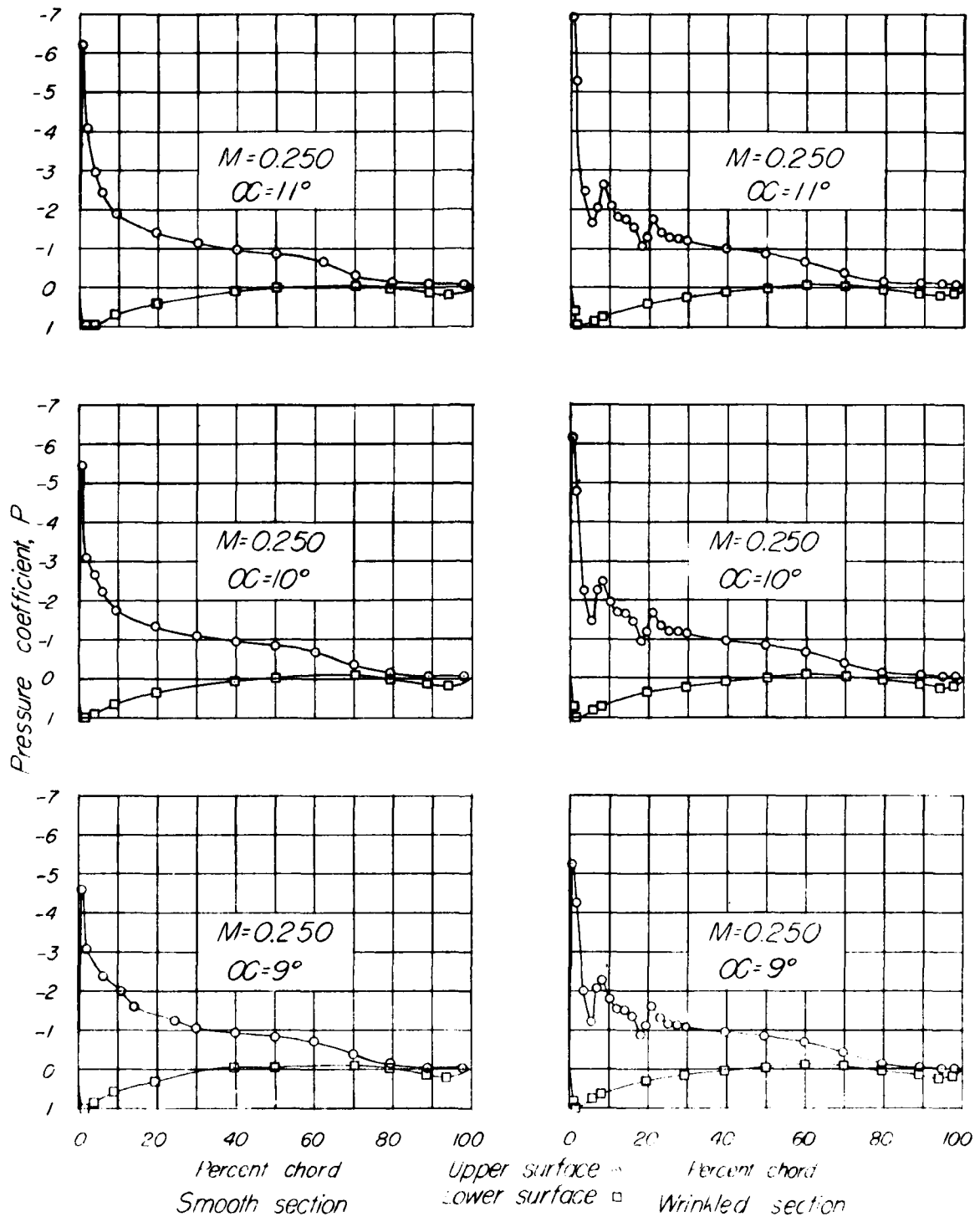
Figure 11.-Pressure distribution over NACA 66,1-115 airfoil.
α = 9°, 10°, and 11°

Fig. 12   NACA TN No. 1121
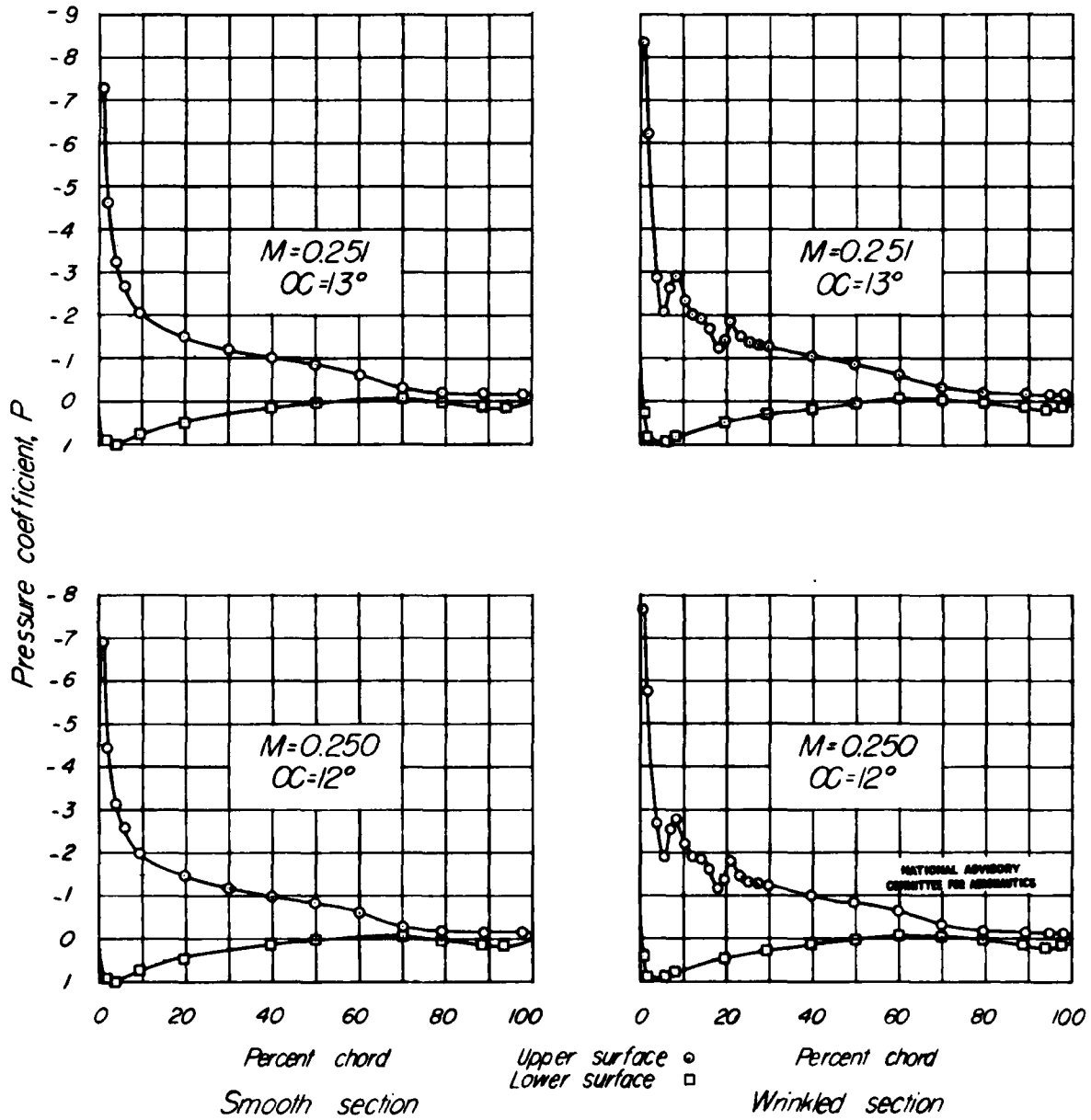
Figure 12.-Pressure distribution over NACA 66,1-115 airfoil.
α = 12° and 13°
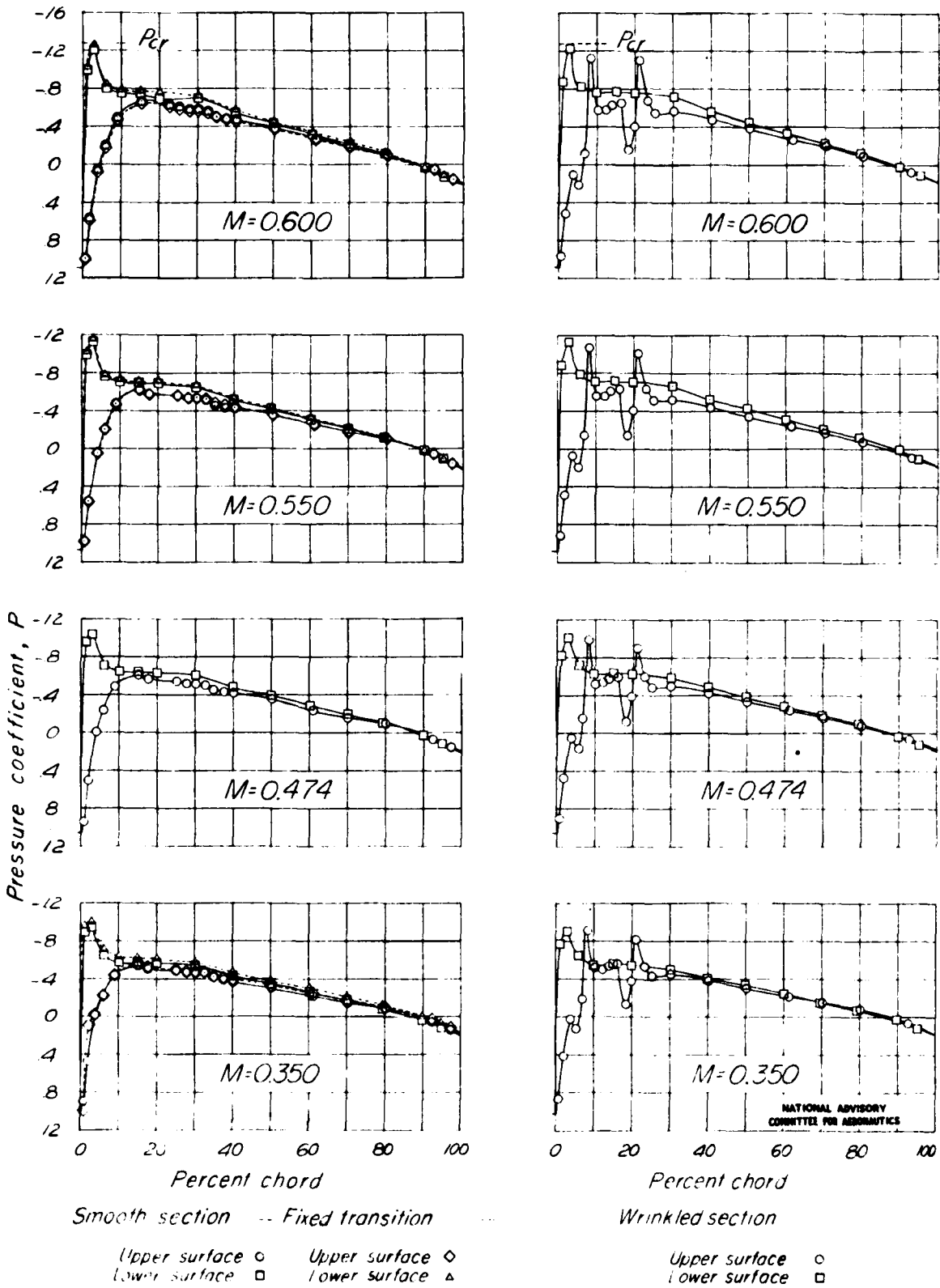
Figure 13.—Pressure distribution over NACA 23015 airfoil. $\alpha = -2.°$

Fig. 13 conc.   NACA TN No. 1121

Figure 13. Concluded
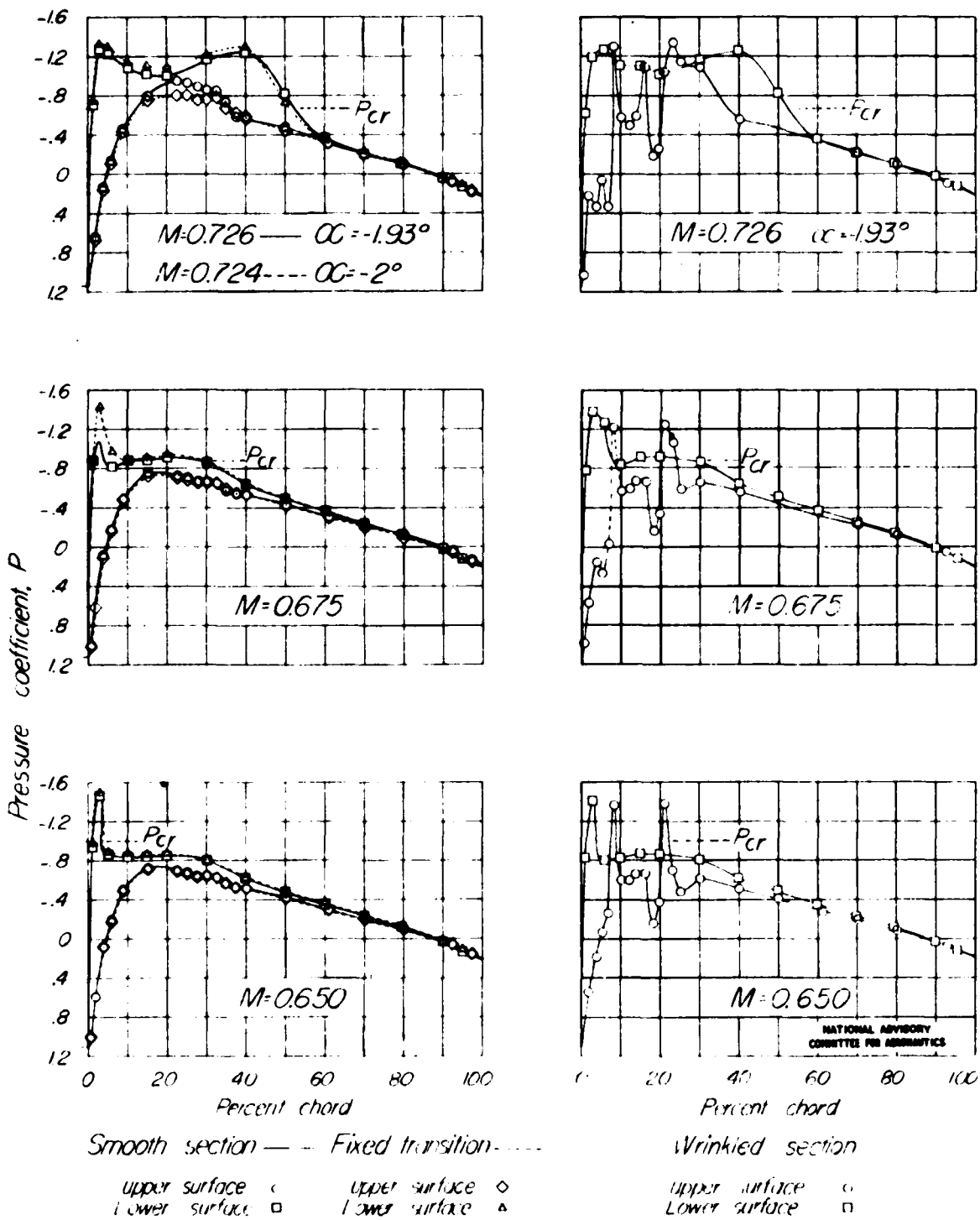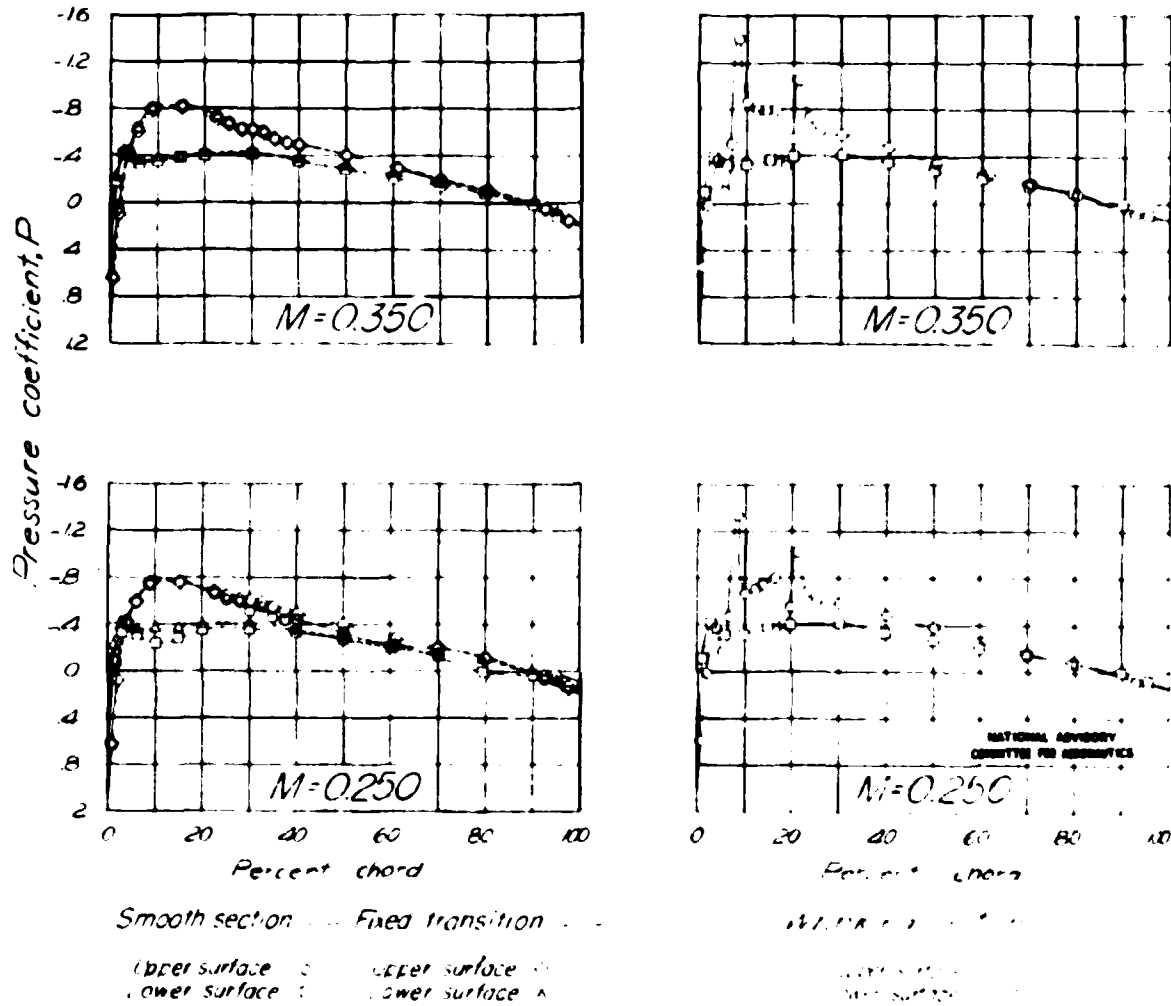
Figure 14 - Pressure distribution over NACA 23015 airfoil $\alpha = 0^\circ$

Fig. 14 cont.

NACA TN No. 1121

Figure 14.- Continued.
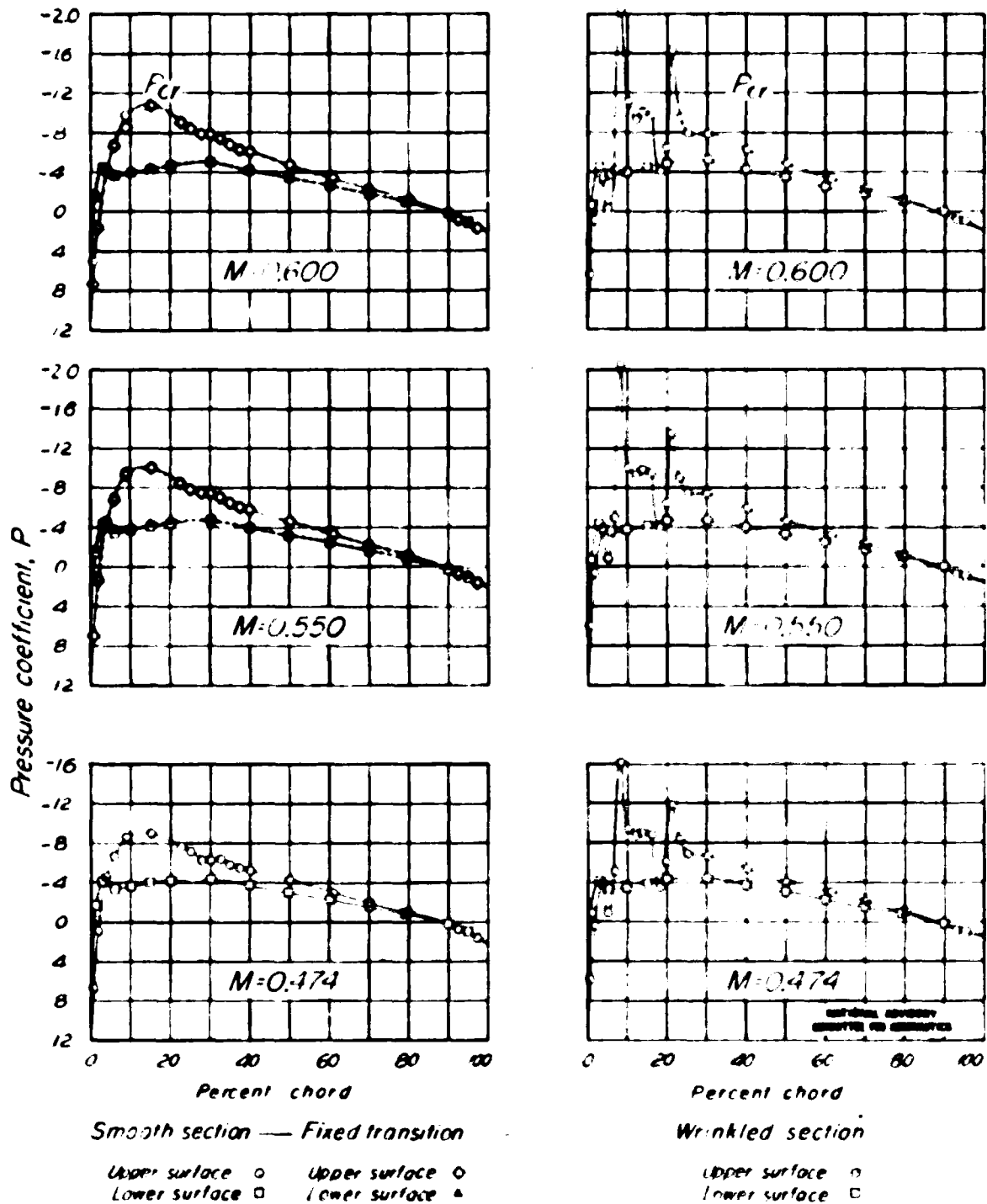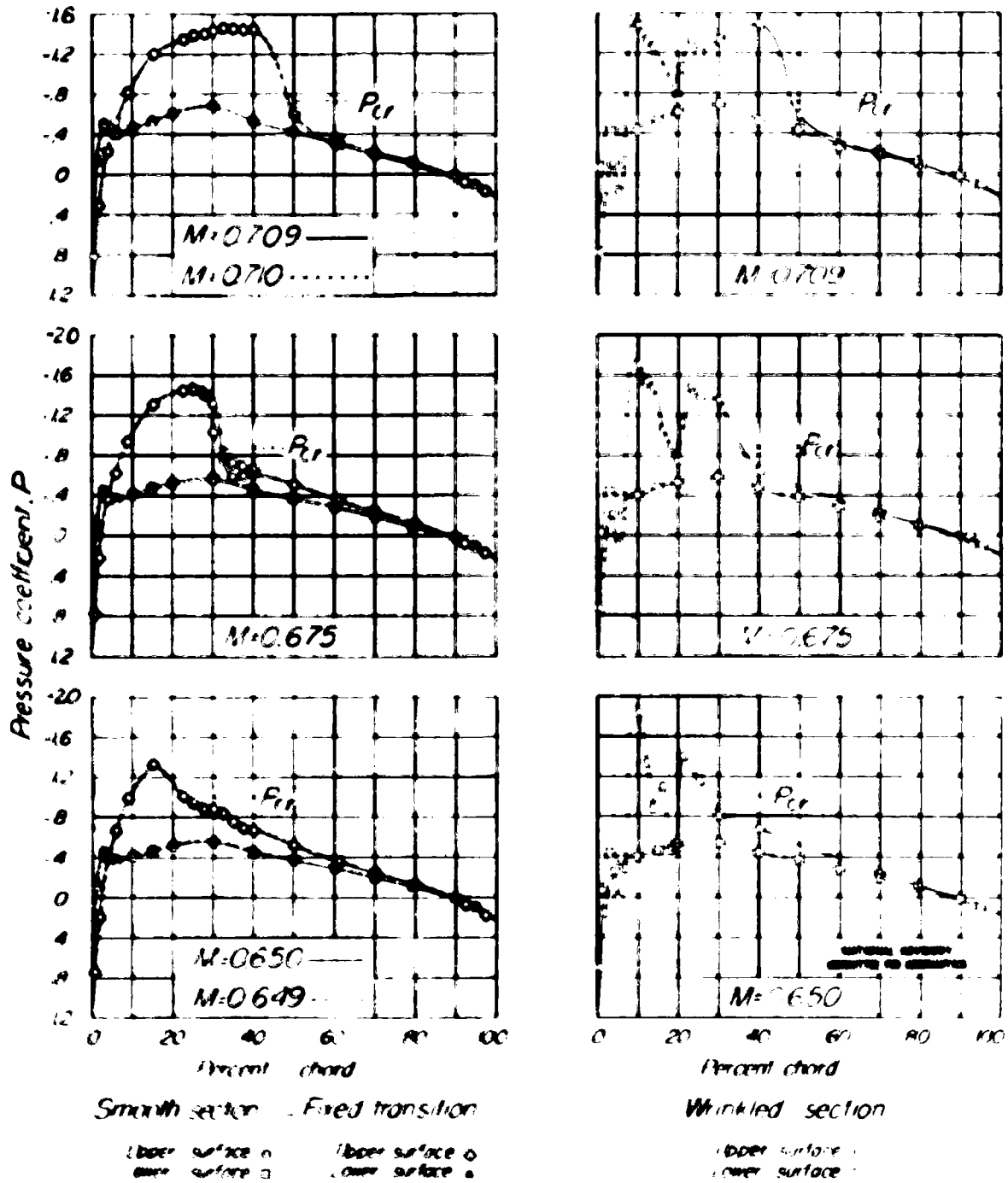
Figure 14 - Concluded

Fig. 15   NACA TN No. 1121
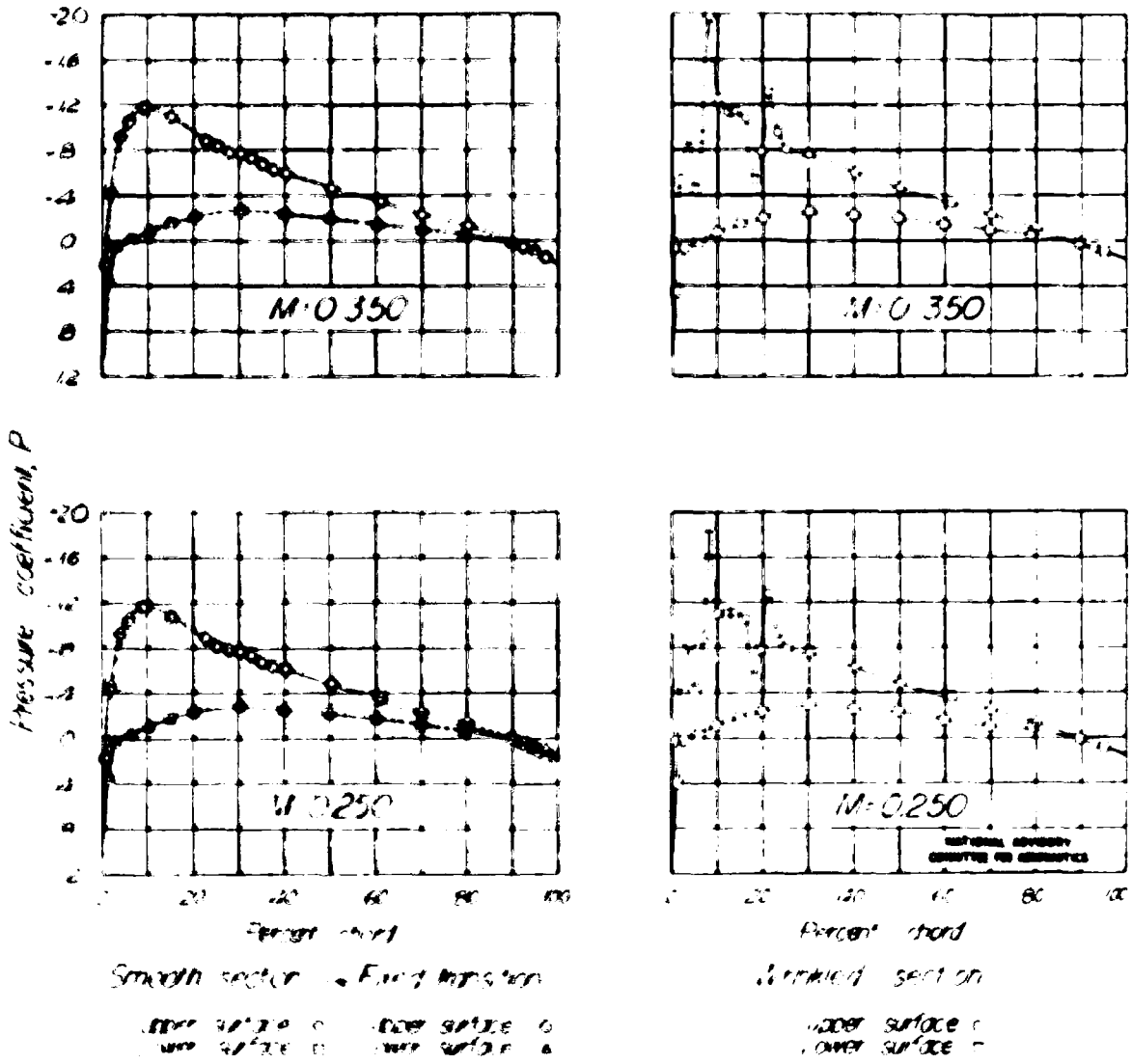
Figure 15.- Pressure distribution over NACA 23015 airfoil. α = 2°

Figure 15. - Continued.

Fig. 15 conc.   NACA TN No. 1121
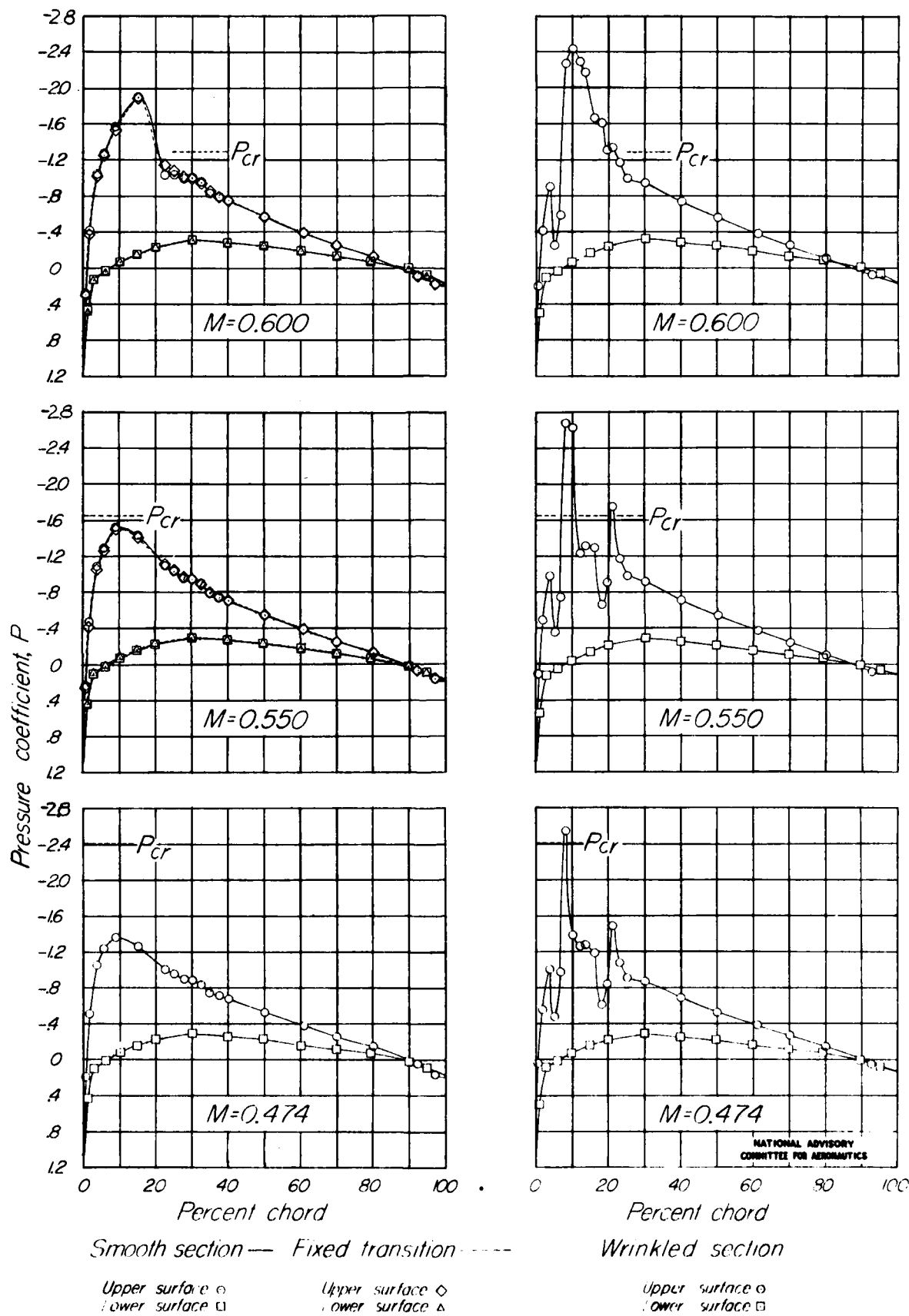
Smooth section — Fixed transition ----

Upper surface ⊙   Upper surface ◇
Lower surface □   Lower surface ▲

Wrinkled section

Upper surface ⊙
Lower surface ⊡
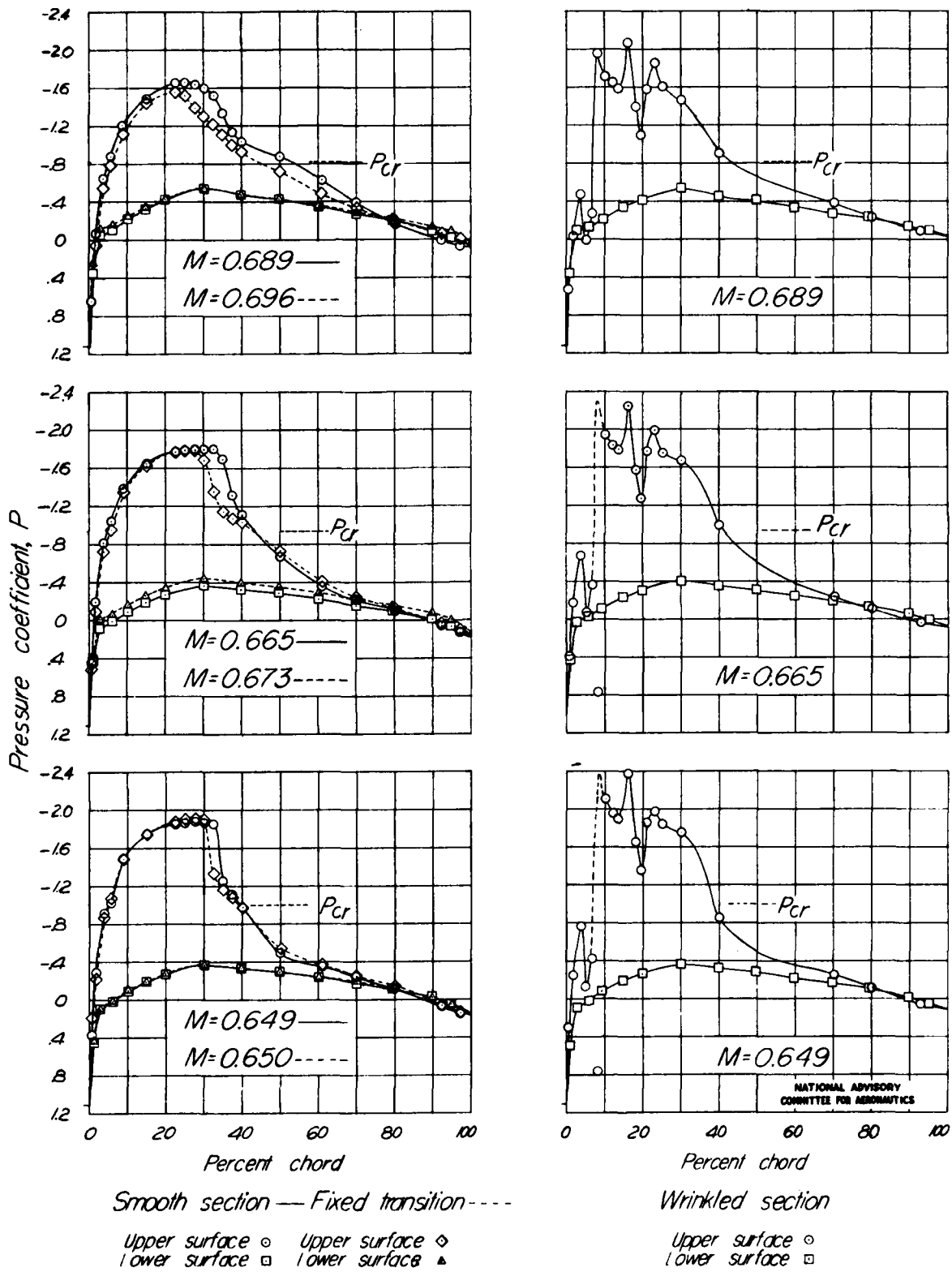
Figure 15.-Concluded.
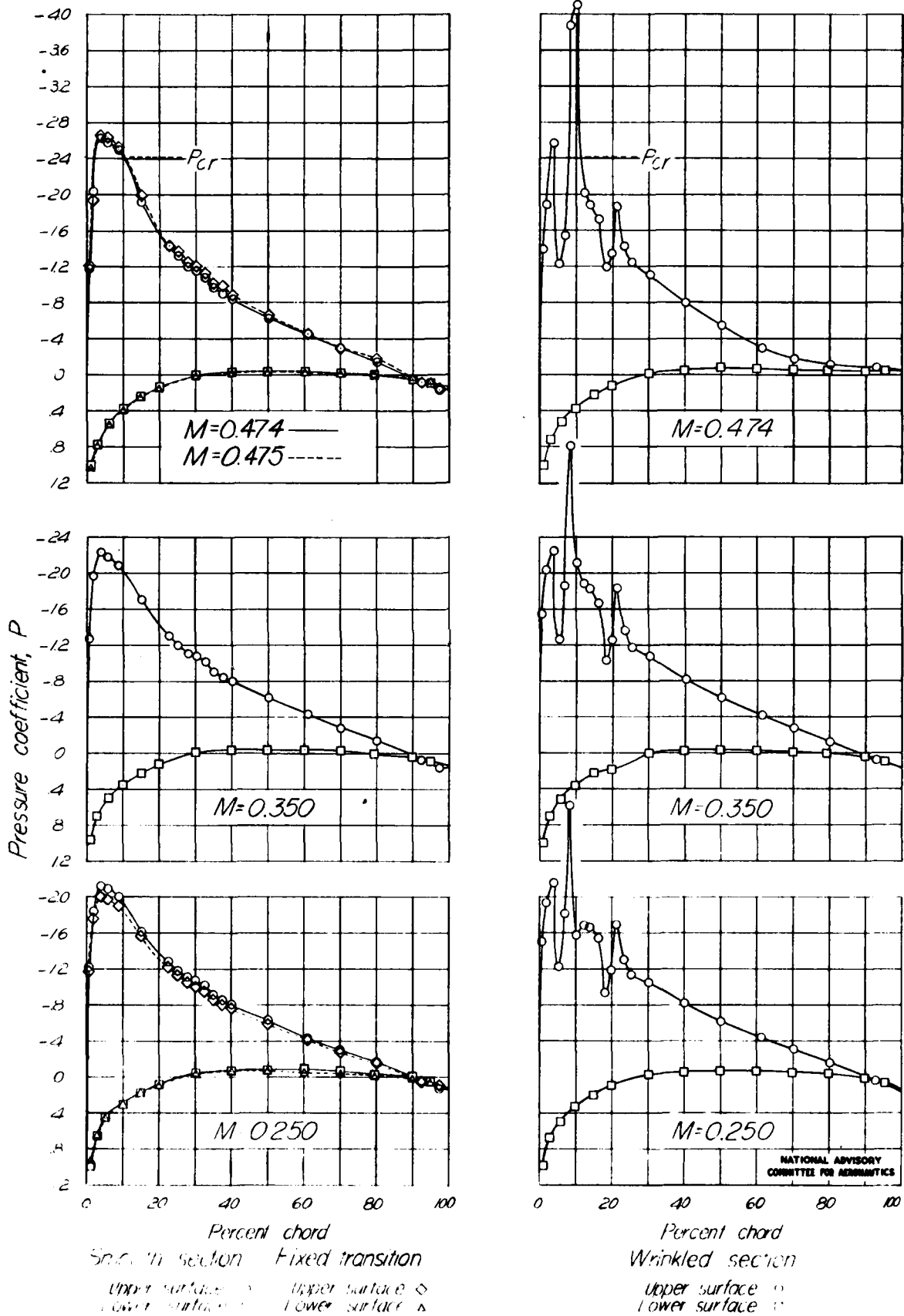
Figure 16.—Pressure distribution over NACA 23015 airfoil. α = 6.°

Fig. 17   NACA TN No. 1121
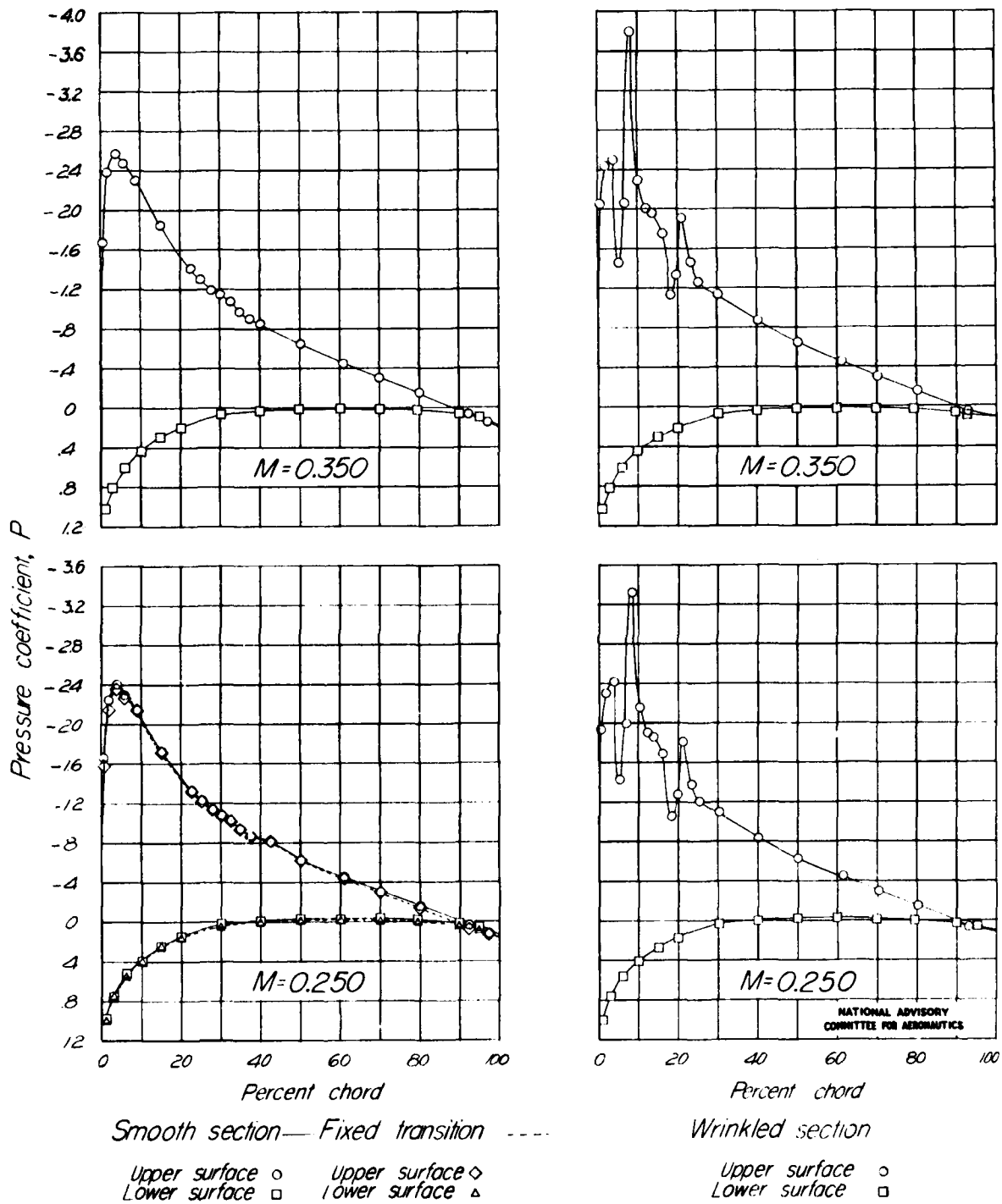
Figure 17.-Pressure distribution over NACA 23015 airfoil. ⍺=7°

Fig. 18
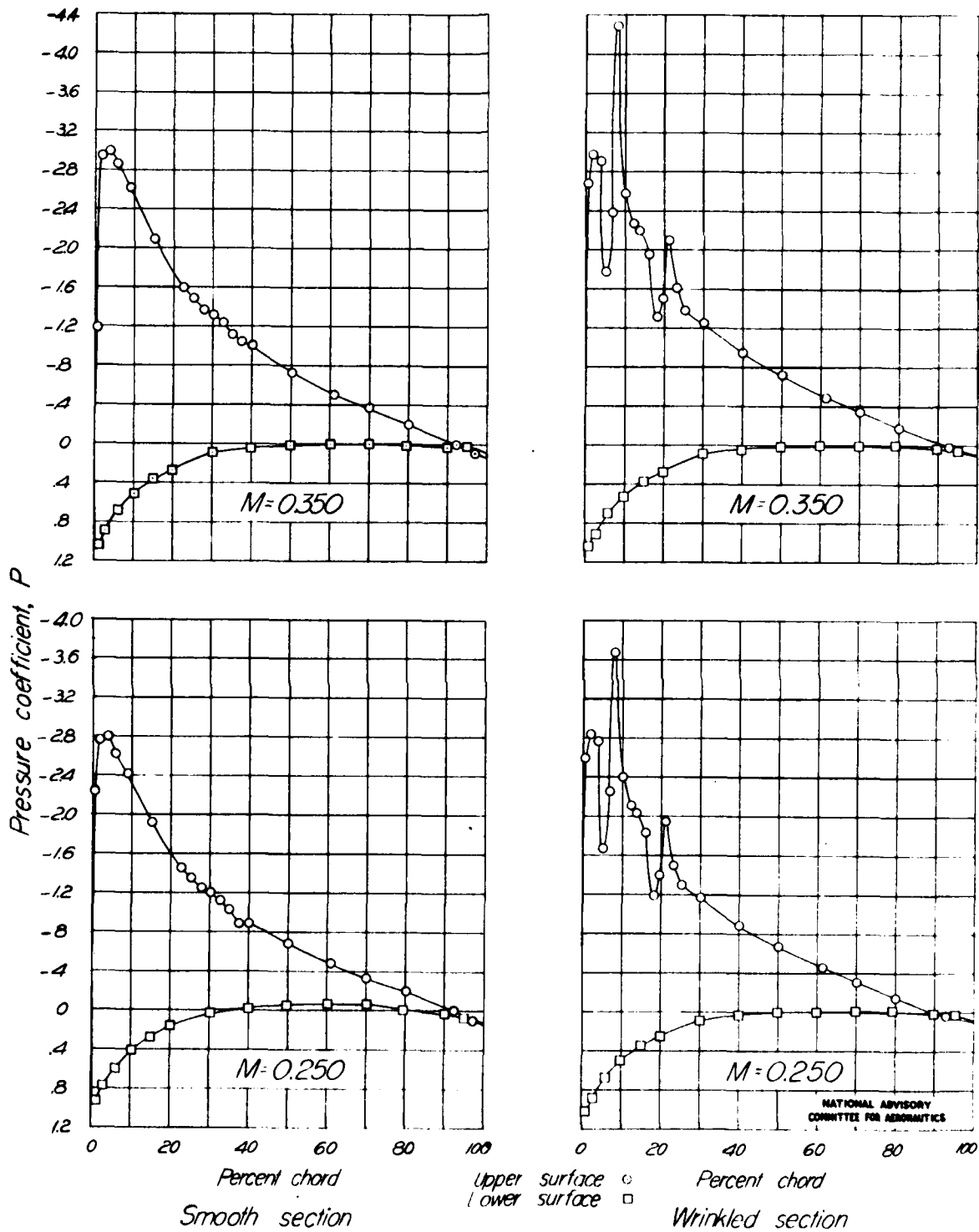
Figure 18.-Pressure distribution over NACA 23015 airfoil. $\alpha = 9.°$

Fig. 19   NACA TN No. 1121
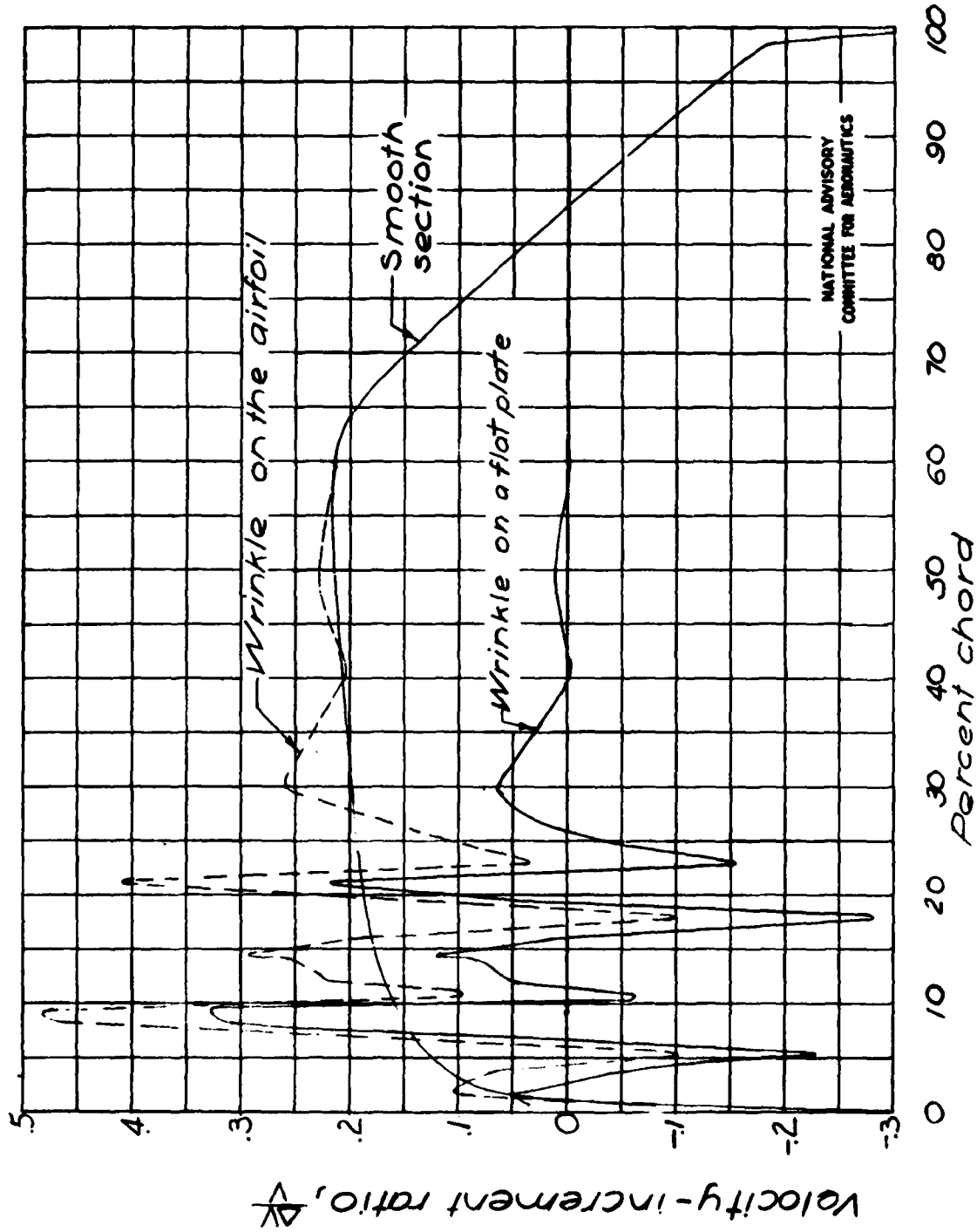
Figure 19. — Theoretical velocity distribution over the upper surface of the smooth NACA 66,1-115 airfoil ($\alpha = 0^\circ$, $M = 0.250$) and over the wrinkle on a flat plate and on the airfoil ($\alpha = 0^\circ$).
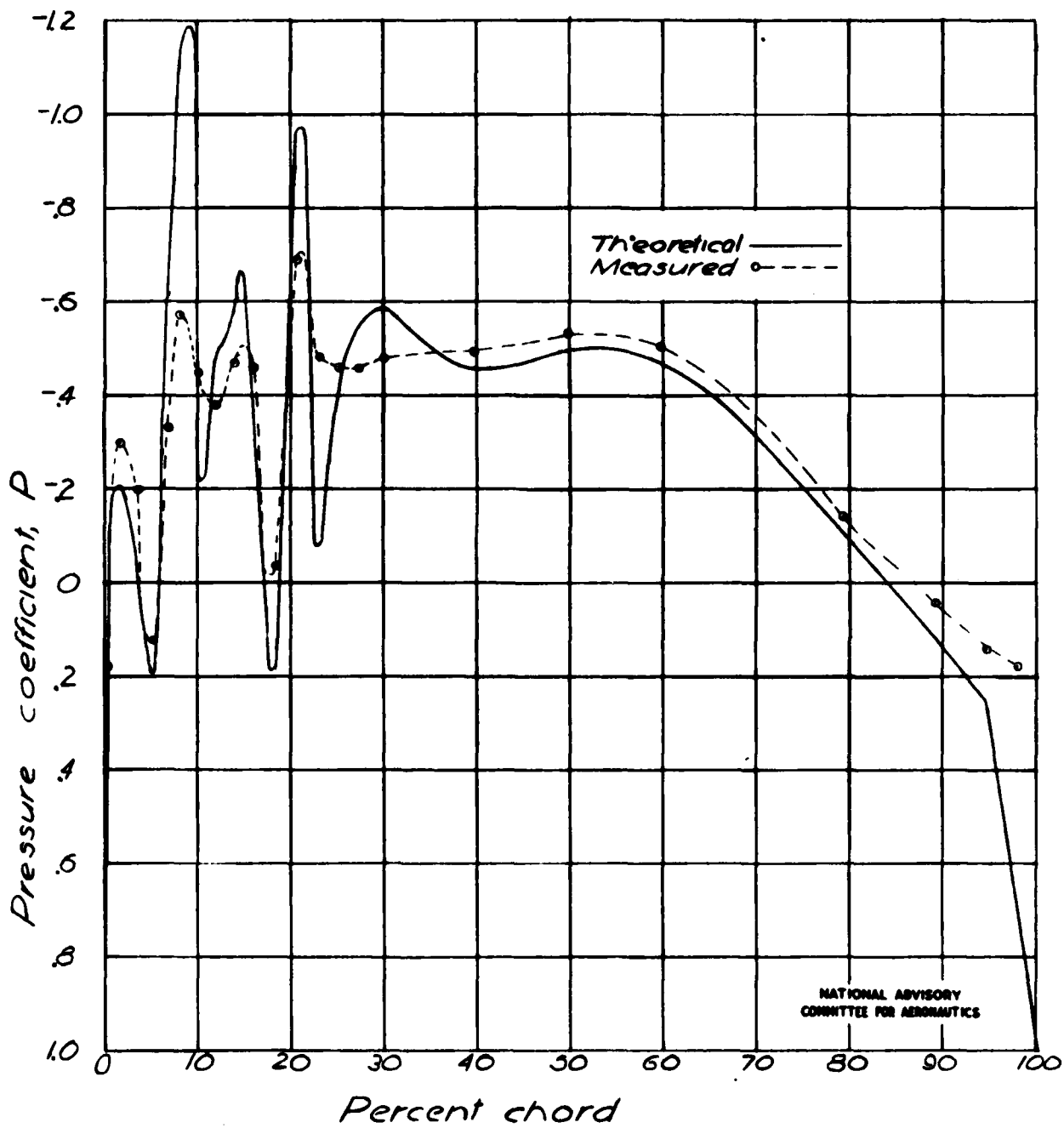
Figure 20.- Comparison of theoretical and measured pressure distribution over upper surface of the NACA 66,1-115 airfoil. M = 0.250, α = 0°.

Fig. 21   NACA TN No. 1121
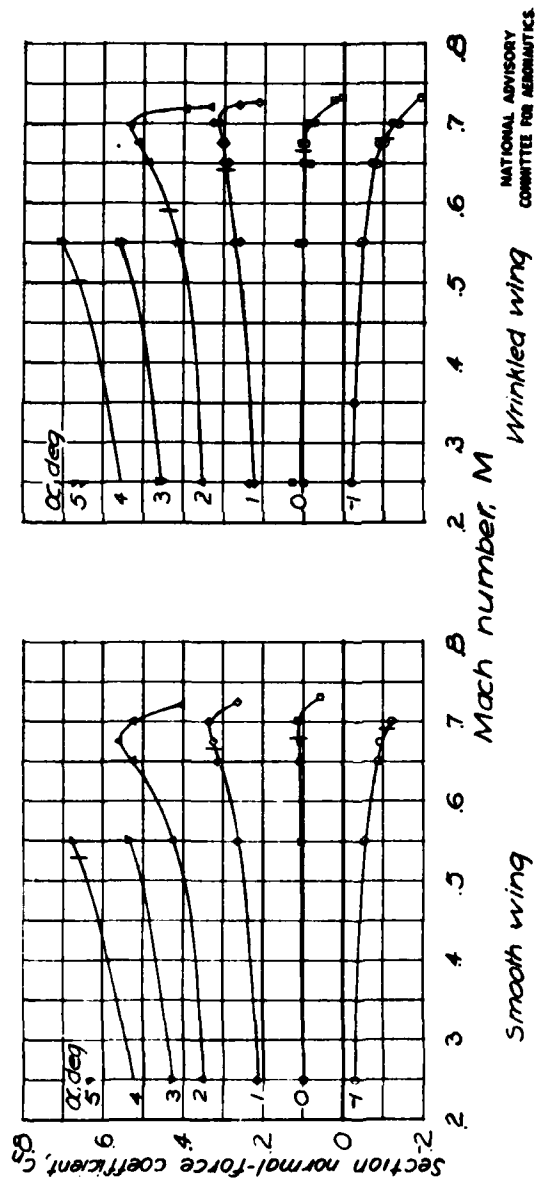
Figure 21.- Variation of normal-force coefficient with Mach number. NACA 66,1-115 airfoil. (Ticks indicate the critical speed.)
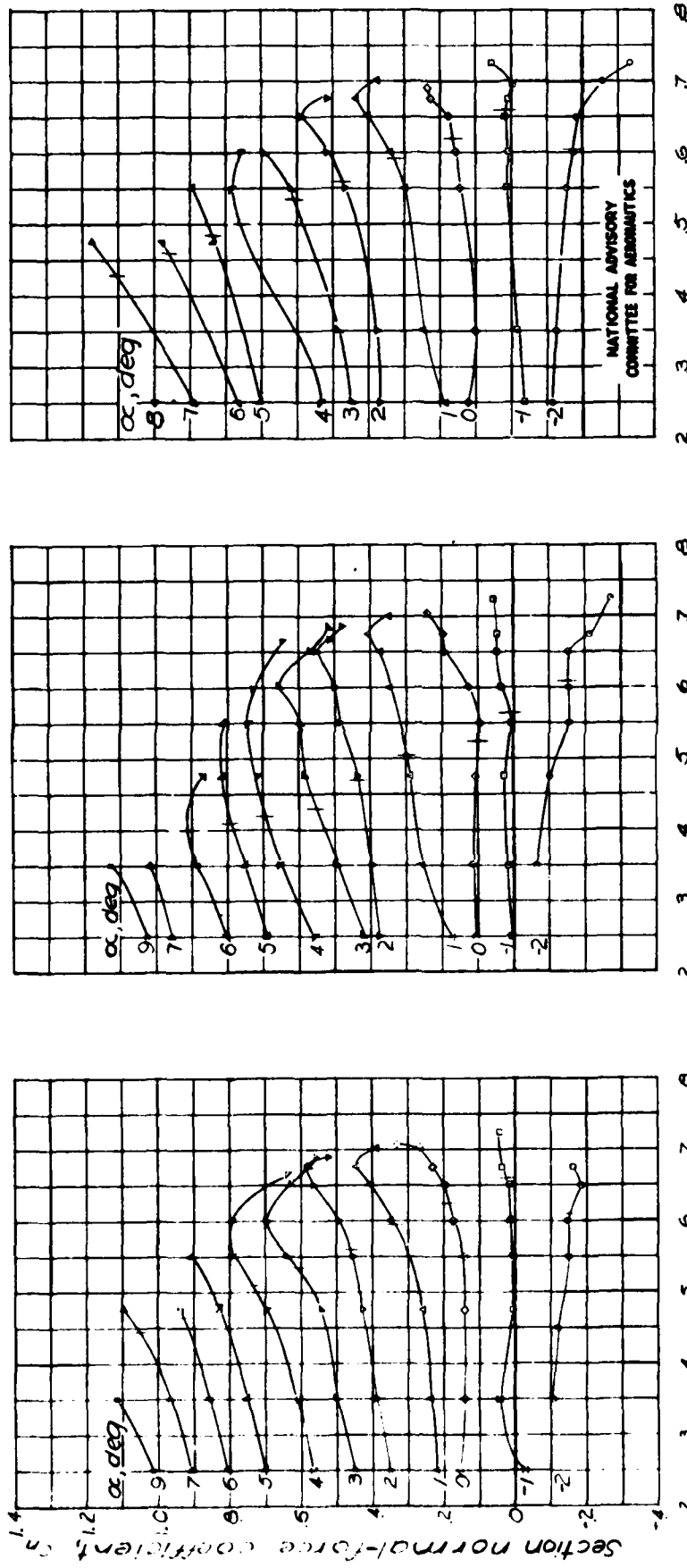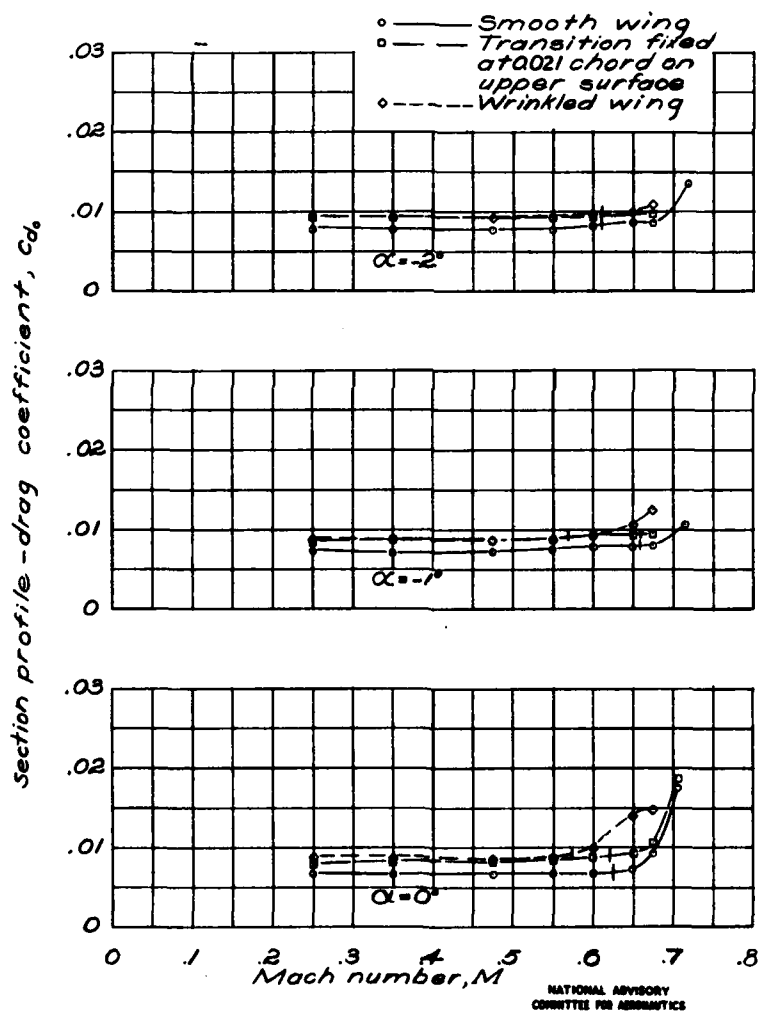
Figure 22. — Variation of section normal-force coefficient with Mach number. NACA 23015 airfoil. (Ticks indicate the critical speed)

Fig. 23   NACA TN No. 1121
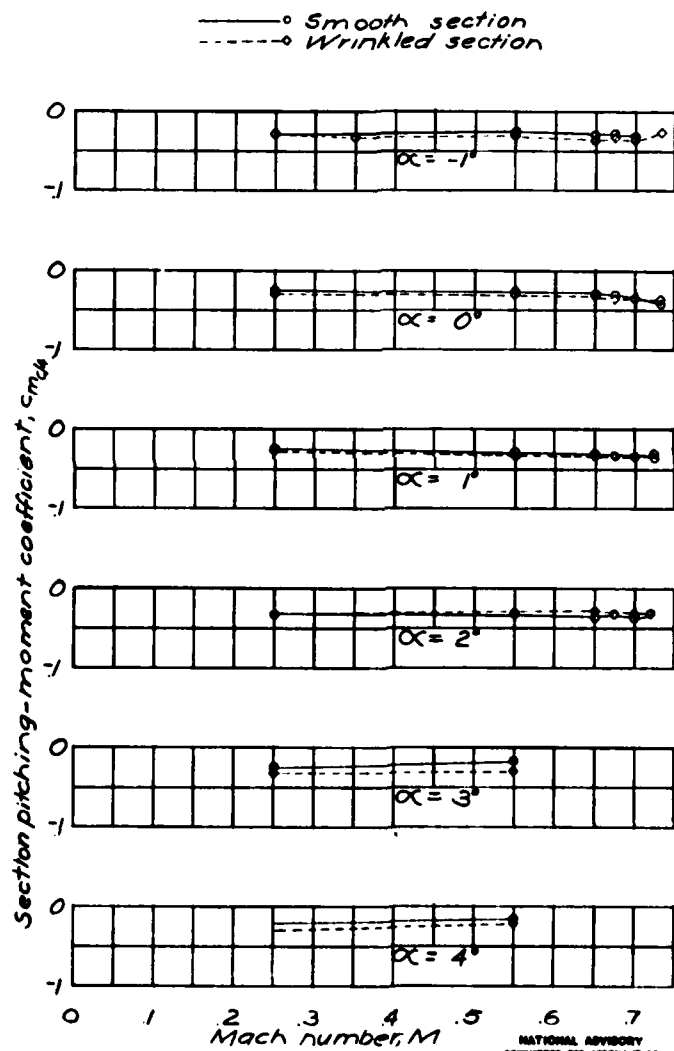
Figure 23.— Variation of section pitching-moment coefficient with Mach number. NACA 66,1-115 airfoil.
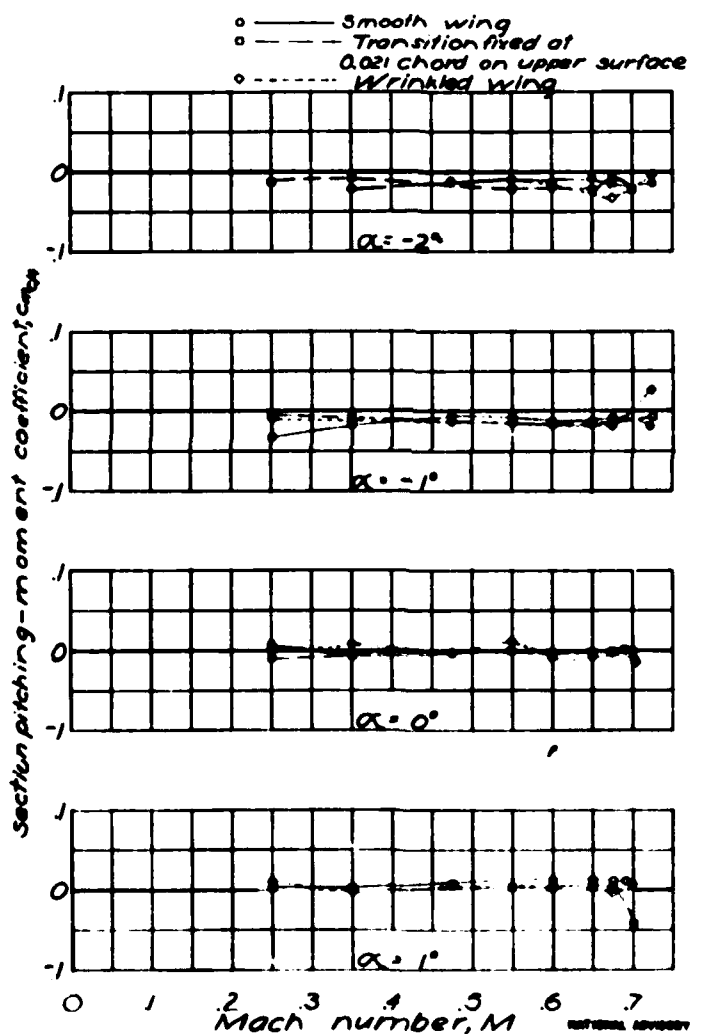
Figure 24 - Variation of section pitching-moment coefficient with Mach number. NACA 23015 airfoil.

Fig. 24 cont. NACA TN No. 1121
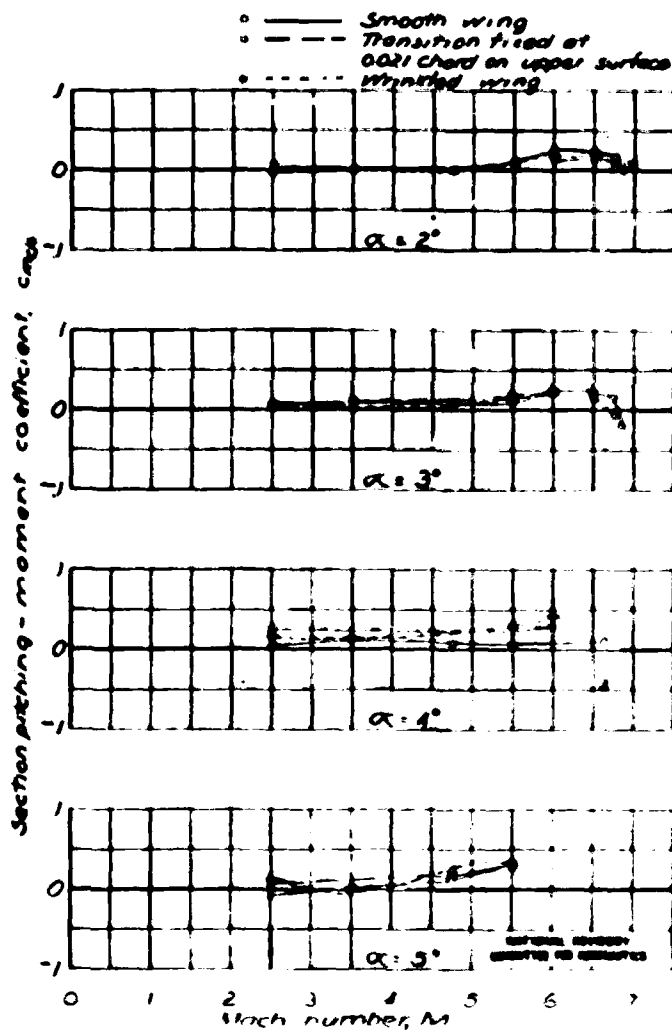
Figure 24.- Continued.
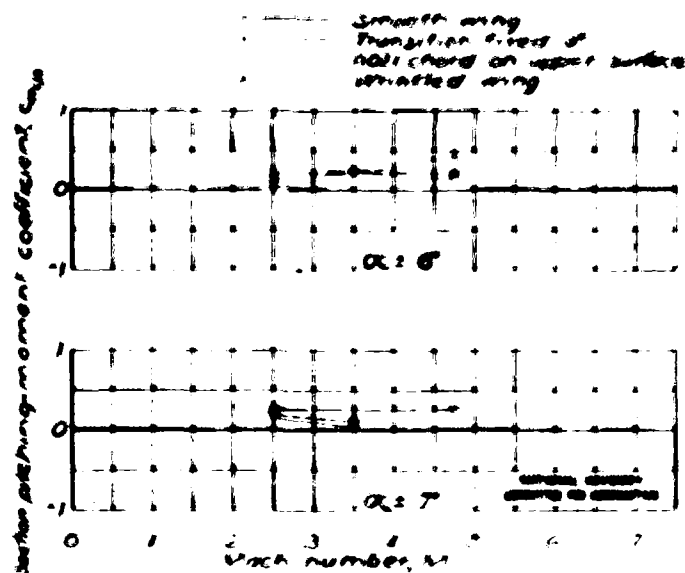
Figure 24.- Concluded.

Fig. 25   NACA TN No. 1121
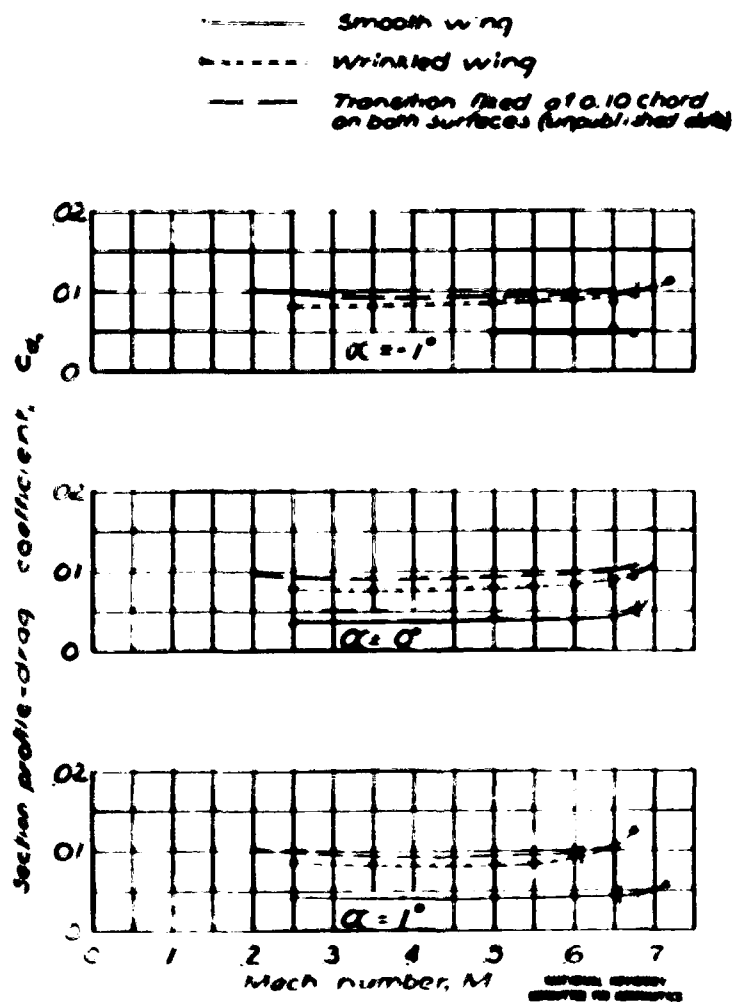
Figure 25 — Variation of section profile-drag coefficient with Mach number NACA 66,-115 airfoil (Ticks indicate the critical speed)
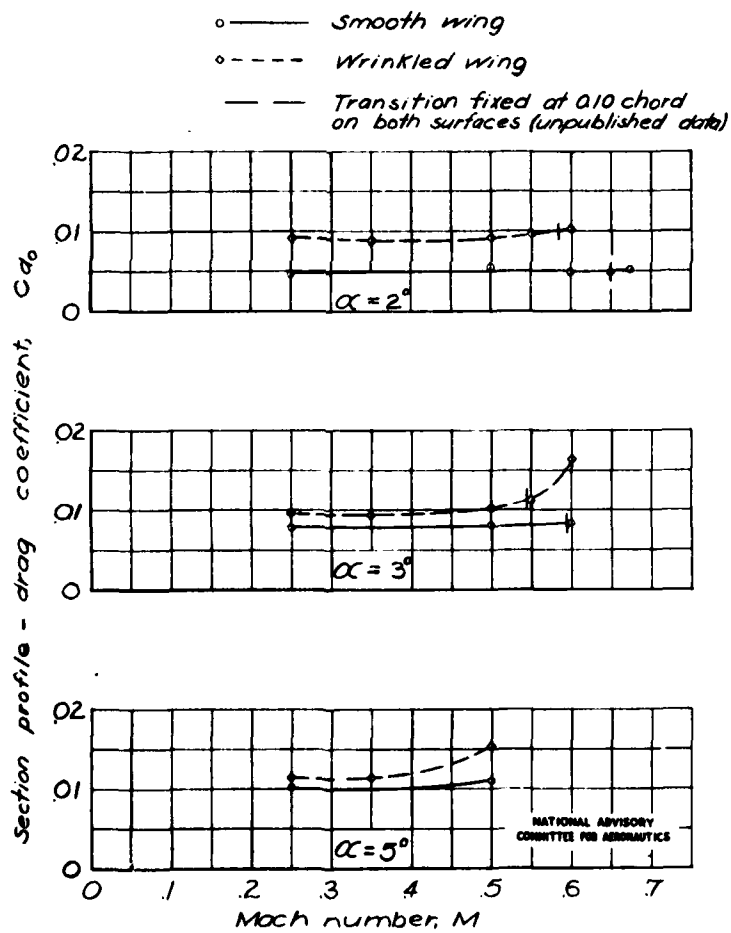
Figure 25 .— Concluded.

Fig. 26

NACA TN No. 1121
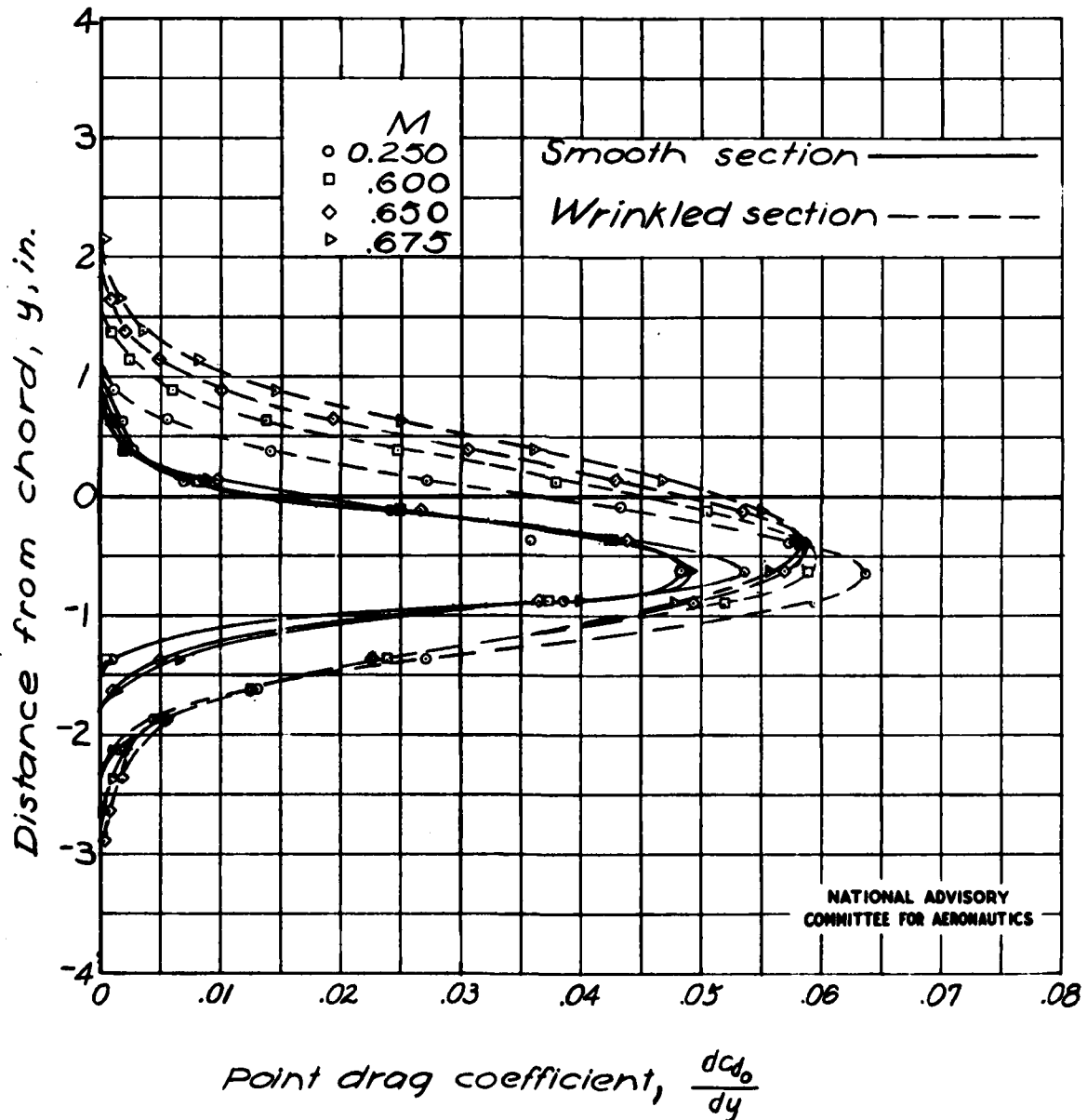

Figure 26.- Variation of section profile-drag coefficient
with Mach number. NACA 23015
airfoil. (Ticks indicate the critical speed.)

Figure 26.- Continued

Fig. 26 conc.   NACA TN No. 1121
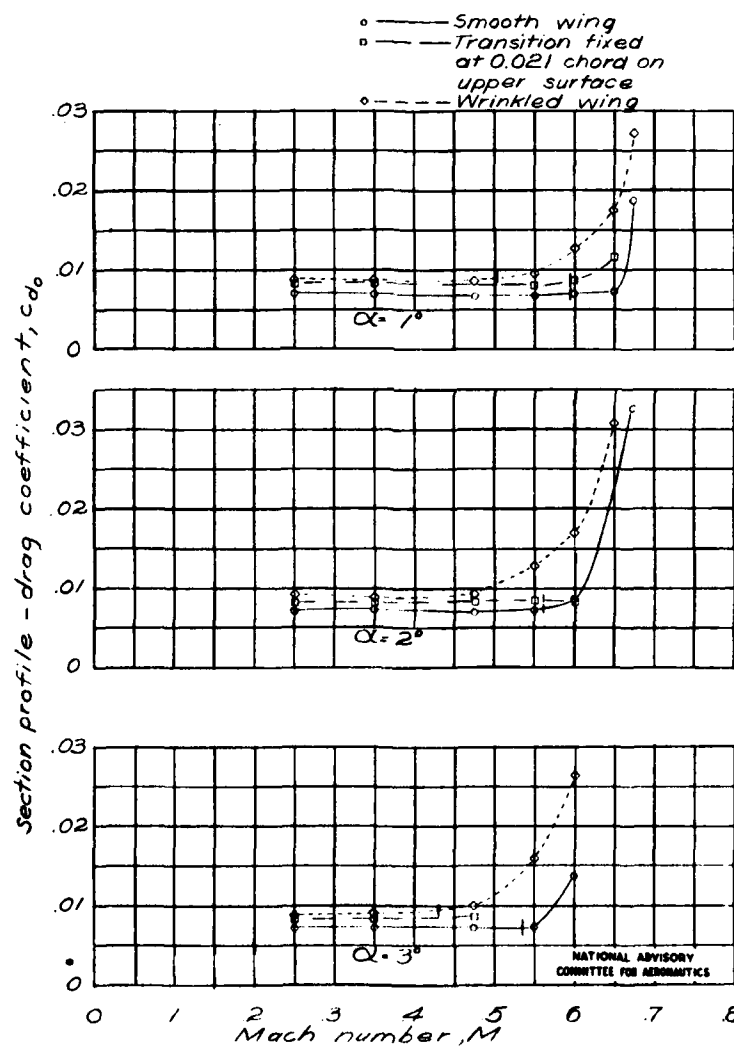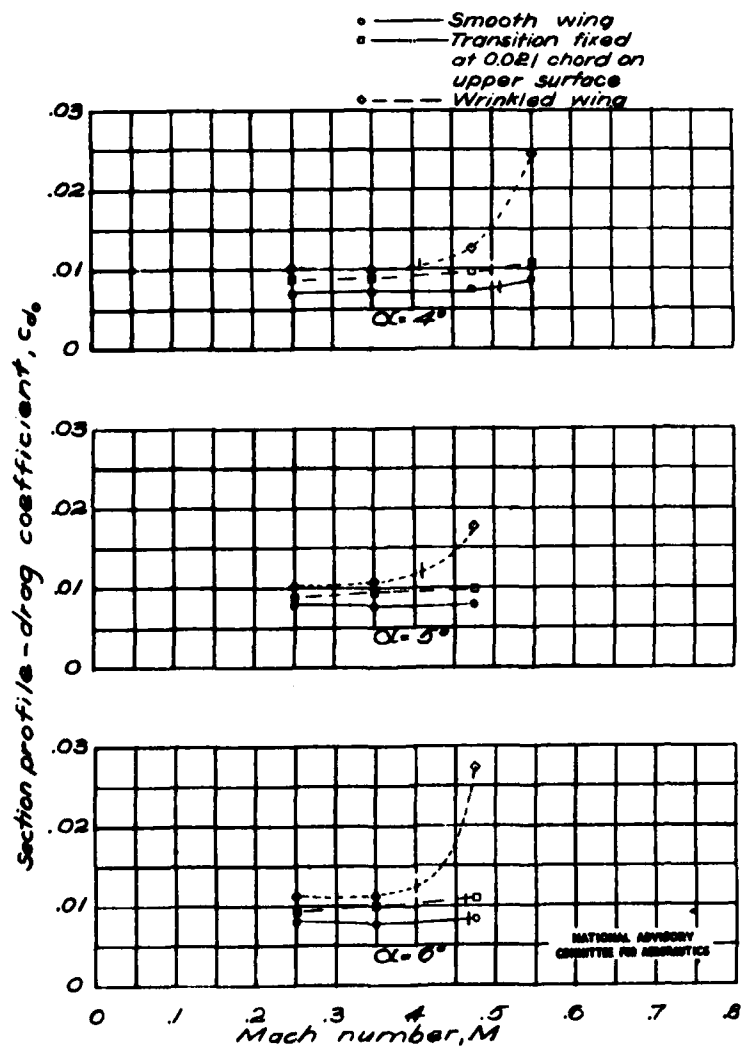
Figure 26.— Concluded.

Figure 27 .— Typical point drag coefficient (total-pressure loss) 1.54 chords behind the trailing edge of the NACA 66,1-115 airfoil. $\alpha = 0°$.
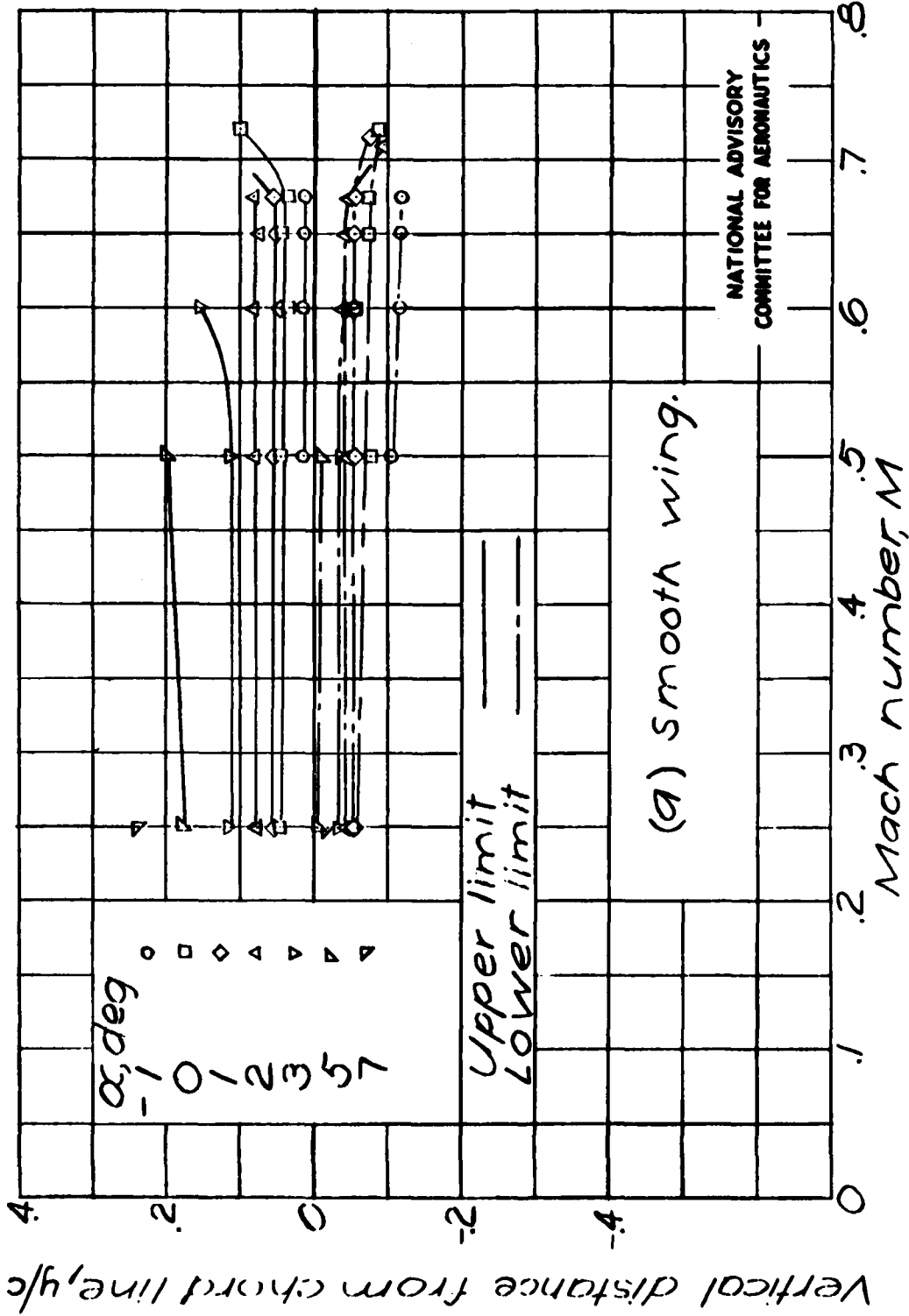
Fig. 28   NACA TN No. 1121

Figure 28.- Wake location 1.54 chords behind trailing edge of NACA 66,1-115 airfoil.

(a) Smooth wing.

(b) Wrinkled wing.
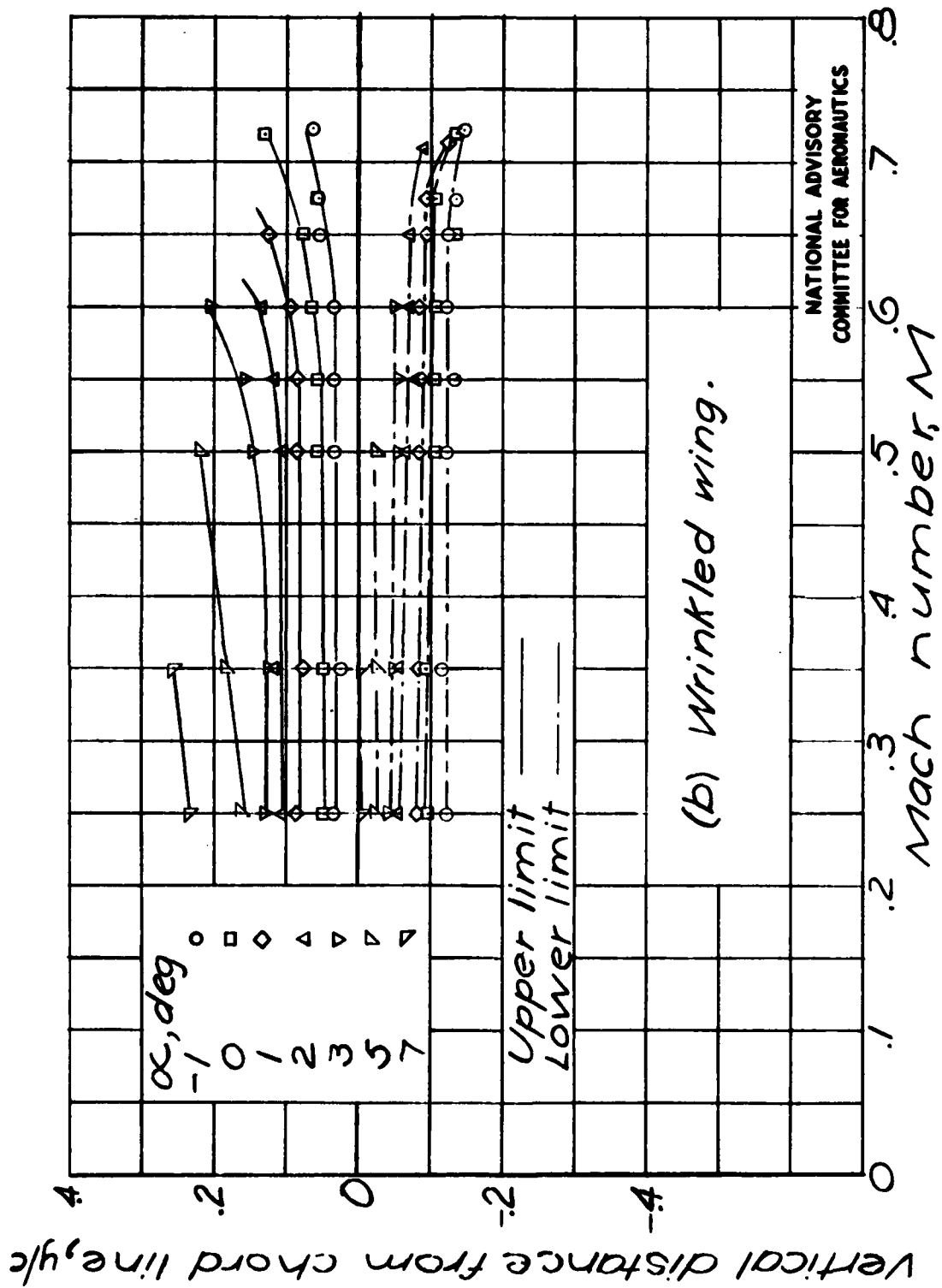
Figure 28.- Concluded.

Fig. 29   NACA TN No. 1121

Figure 29. – Wake location 0.826 chord behind trailing edge
of NACA 23015 airfoil.

(b) Wrinkled wing.
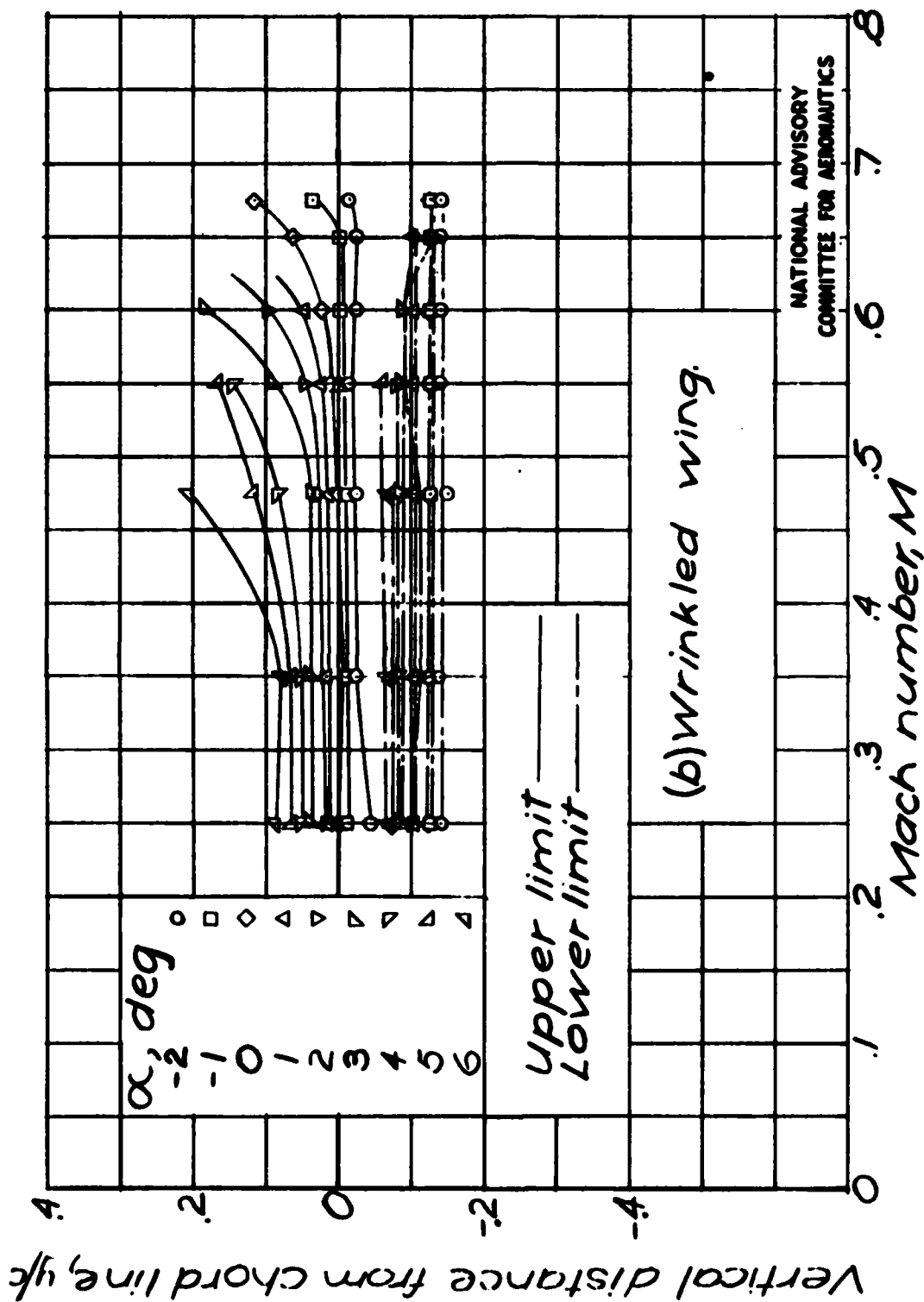
Figure 29.- Continued.

Fig. 29 conc.   NACA TN No. 1121

(c) Transition fixed on upper surface at 0.021 chord.

Figure 29.- Concluded.

(a) NACA 66,1-115 airfoil.

(b) NACA 23015 airfoil.
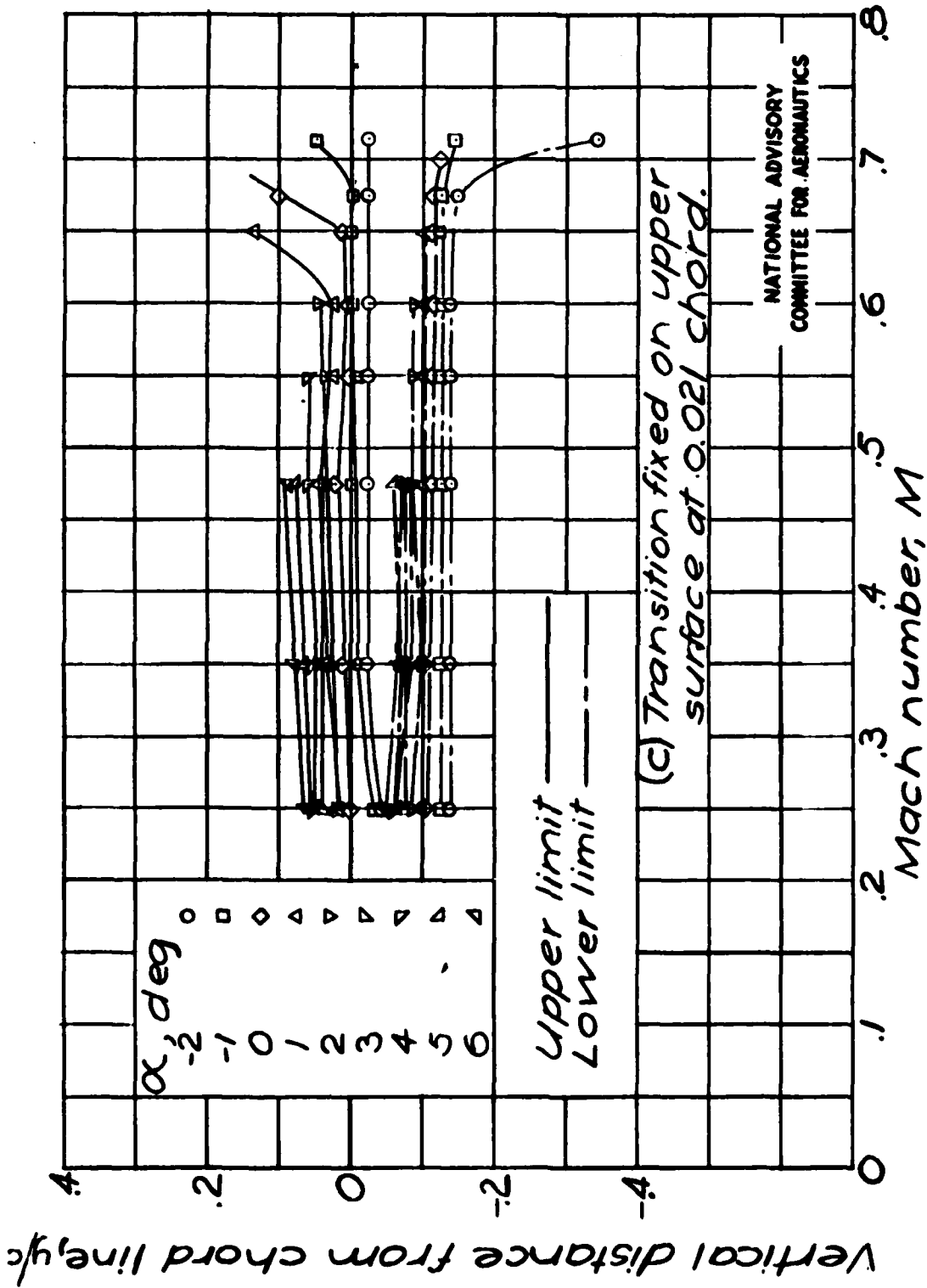
Figure 30.- Variation of critical Mach number with section normal-force coefficient.

ORIG. AGENCY NUMBER

TN-1121

REVISION

DIVISION: Aerodynamics (2)
SECTION: Wings and Airfoils (6)
CROSS REFERENCES: Wings - Aerodynamics (99150); Drag, Aerodynamic (31080)

AUTHOR(S): Robinson, H. L.

AMER. TITLE: High-speed investigation of skin wrinkles on two NACA airfoils

FORG'N. TITLE:

ORIGINATING AGENCY: National Advisory Committee for Aeronautics, Washington, D. C.

TRANSLATION:

COUNTRY	LANGUAGE	FORG'N.CLASS	U.S.CLASS.	DATE	PAGES	ILLUS.	FEATURES
U.S.	Eng.		Unclass.	Aug'46	63	47	photo, table, diagrs, drwgs

ABSTRACT

The effects on the aerodynamic characteristics of skin wrinkles on the forward part of the upper surface of two NACA airfoils, the NACA 66, 1-115 and 23015 sections, at speeds up to Mach number 0.73 were investigated and the results compared with those obtained for the same two airfoils under smooth conditions. No appreciable change in normal-force or pitching-moment characteristics was caused by the wrinkle on an airfoil section. The drag was greater for the wrinkled configuration than for the smooth one.

NOTE: Requests for copies of this report must be addressed to: N.A.C.A., Washington, D. C.

I-2, HQ., AIR MATERIEL COMMAND   AIR TECHNICAL INDEX   WRIGHT FIELD, OHIO, USAAF